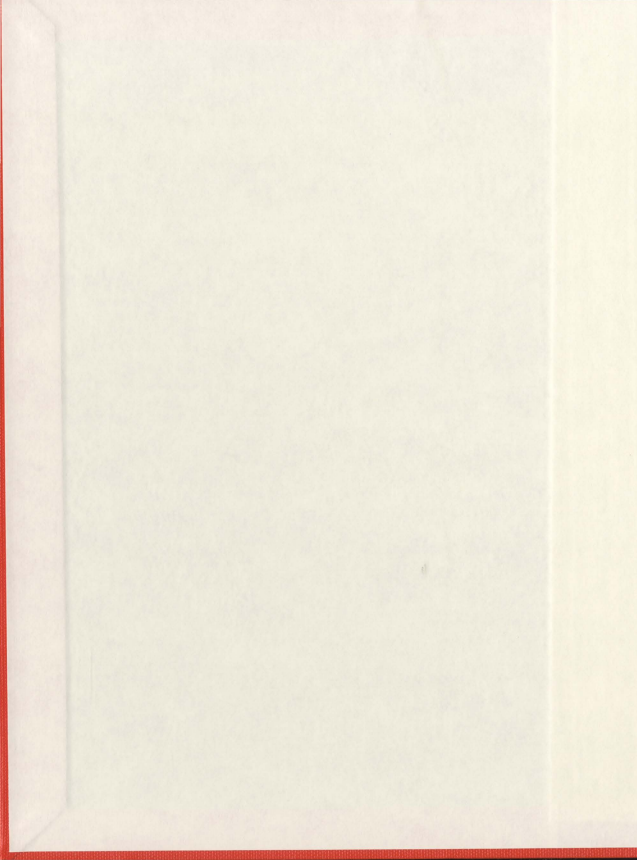


EXPERIMENTAL DETERMINATION OF EQUIVALENT
CIRCUIT PARAMETERS FOR A LABORATORY
SALIENT-POLE SYNCHRONOUS GENERATOR

DAW GHANIM



**EXPERIMENTAL DETERMINATION OF EQUIVALENT CIRCUIT
PARAMETERS FOR A LABORATORY SALIENT-POLE SYNCHRONOUS
GENERATOR**

by

© Daw Ghanim



A thesis

submitted to the School of Graduate Studies

in partial fulfillment of the requirements for the degree of

MASTER OF ENGINEERING

Faculty of Engineering and Applied Science
Memorial University of Newfoundland

September 2012

St. John's, Newfoundland, Canada

ABSTRACT

Nearly all of the electric energy used for numerous applications in today's world, regardless of the assembly of the used prime movers, is generated by means of synchronous generators. These generators can be connected together in small-scale or large-scale generation power systems depending on the load demand. Indeed, it is of utmost necessity to pay serious attention to those electric machines, their performance characteristics, various operation conditions and their design parameters. One of the most important parameters of the synchronous generator that can be a good asset for synchronous machines designers is the synchronous reactance. The importance of this reactance lies in the significant role it plays in the quality of the produced electric power and thus the stability of the voltage obtained across the terminals of a synchronous generator. The synchronous reactance of a synchronous generator may have different values based on the mode of the operation or the loading conditions. The primary purpose of this thesis is to determine the direct-axis synchronous reactance values as well as the identification of stator leakage reactance of a real synchronous generator from the so-called *Potier triangle method*. A set of standard tests based on the *IEEE standard 115* is set forth and conducted on the machine under test which is a laboratory synchronous generator of a salient-pole type, or so-called hydroelectric or waterwheel generator. The experimental test data and results are provided and analyzed with full details, and then the relevant machine parameters are calculated at the end of this thesis.

ACKNOWLEDGEMENTS

I have been indebted in the preparation of this thesis to my supervisor Dr. M. A. Rahman for his patience, kindness and invaluable guidance and encouragement. I am also truly grateful to the School of Graduate Studies and Faculty of Engineering and Applied Science at Memorial University of Newfoundland for the considerable effort they made to facilitate my study at MUN. At this point, special thanks go to Ms. Moya Crocker and Ms. Colleen Mahoney at the Office of the Associate Dean at the Faculty of Engineering and Applied Science. I would like to acknowledge my fellow graduate students for their useful suggestions during various stages of this research work.

Furthermore, I am truly grateful to the Ministry of Higher Education and Scientific Research of Libya for financially supporting my study in Canada. Also, the considerable effort made by the Canadian Bureau for International Education (CBIE), especially by my Academic Manager Ms. Diane Cyr., is indeed highly acknowledged.

Finally, my great thanks go to my parents, brother and sisters for being sustainable sources of inspiration all through my life. It is to them this thesis is dedicated.

Table of Contents

Abstract.....	ii
Acknowledgements.....	iii
Table of Contents.....	iv
List of Figures.....	vii
List of Tables.....	ix
List of Symbols.....	x
List of Abbreviations.....	xiii
Chapter 1: Introduction.....	1
1.1 General Background.....	1
1.2 Literature Review.....	3
1.2.1 Historical Overview of the Two-Axis (dq-Axis) Theory.....	3
1.2.2 Determination of Synchronous Machine Parameters.....	7
1.3 Thesis Objectives.....	14
1.4 Outline of the Thesis.....	14
Chapter 2: Rotating AC Machinery Fundamentals.....	16
2.1 Basics of Magnetic Circuits.....	16
2.2 Induced Voltage Equation.....	19
2.3 Rotating Magnetic Field in AC Machinery.....	23

Chapter 3: Analysis of Synchronous Generator	30
3.1 Brief Overview	30
3.2 Physical Construction	31
3.2.1 The Stator	31
3.2.2 The Rotor	32
3.3 Principle of Operation	33
3.4 Equivalent Circuit of Synchronous Generator	34
3.4.1 Armature Reaction	36
3.4.2 Equivalent Circuit Representation Including Armature Reaction	36
3.5 Effect of Load Changes on the Excitation	39
3.5.1 Lagging Power Factor Load	41
3.5.2 Unity Power Factor Load	42
3.5.3 Leading Power Factor Load	42
3.6 D-Q Axis Analysis of Salient-Pole Synchronous Generator	43
3.6.1 Flux and MMF Waveforms in a Salient-Pole Synchronous Generator	43
3.6.2 Phasor Diagram Representation	46
3.6.3 Steady-State Power-Angle Characteristic	50
3.7 Synchronous Generator Transients.	53
3.7.1 Steady-State Direct-Axis and Quadrature-Axis Synchronous Reactances (X_d and X_q)	54
3.7.2 Direct-Axis Transient and Subtransient Synchronous Reactances (X'_d and X''_d)	55

3.7.3	Quadrature-Axis Transient and Subtransient Synchronous Reactances (X'_q and X''_q).....	57
3.8	Potier Reactance Concept.....	58
Chapter 4: Experimental Determination of Synchronous Machine Parameters.....		60
4.1	The Electric Machine under Consideration.....	60
4.2	The Base Impedance	61
4.3	Measurement of Stator Resistance R_s	61
4.4	The Performed Standard Tests	62
4.4.1	Open-Circuit Test.....	62
4.4.2	The Sustained Short-Circuit Test.....	63
4.4.3	The Slip Test	67
4.4.4	Zero Power-Factor Test	70
4.4.5	Sudden Three-Phase Short-Circuit Test.....	75
4.5	Summary	83
Chapter 5: Conclusion and Future Work.....		84
5.1	Conclusion.....	84
5.2	Future Work	84
References.....		86
Appendix A: Constants of Synchronous Machines.....		95
Appendix B: Three-Phase Short-Circuit at 0.6 pu of Rated Terminal Voltage.....		97

List of Figures

Fig. 2.1. (a) Typical magnetic circuit elements, (b) Equivalent circuit diagram.	17
Fig. 2.2. A conductor moving with an angle (θ°) through a magnetic field	20
Fig. 2.3. Schematic diagram of a 2-pole 3-phase ac machine.....	21
Fig. 2.4. Balanced 3-phase current applied to the stator of ac machine	25
Fig. 2.5. Production of the armature (stator) mmf wave in ac rotating machines; (a) Cross-sectional view of 2-pole ac machine, (field windings are not shown), (b)The resultant stator mmf wave with its components.	26
Fig. 2.6. Vector diagram of the resultant mmf wave	27
Fig. 3.1. Basic Stator Scheme for a 2-pole 3-phase synchronous generator.....	32
Fig. 3.2. Elementary rotor structure of 2-pole alternator: (a) cylindrical rotor, (b) salient-pole rotor.....	33
Fig. 3.3. Y-connected 3-phase stator distributed windings of a synchronous machine.....	35
Fig. 3.4. Single-phase equivalent circuit of a cylindrical rotor synchronous generator: (a) including armature reaction effect, (b) comprising the synchronous reactance.	36
Fig. 3.5. Phasor diagram of a cylindrical rotor synchronous generator: (a) lagging power factor load, (b) unity power factor load, (c) leading power factor load.....	40
Fig. 3.6. mmfs distribution in a salient-pole synchronous generator: (a) physical view (only phase-a is shown on the stator), (b) space-fundamental mmf waves with the respective d-q axes.....	45
Fig. 3.7. d-q axis steady-state phasor diagram of a salient pole synchronous generator with lagging power factor load	47

Fig. 3.8. Steady-state power-angle characteristic of a salient-pole synchronous generator	53
Fig. 4.1. Laboratory salient-pole synchronous machine	60
Fig. 4.2. Open- and Short-Circuit Characteristics for the laboratory synchronous generator	65
Fig. 4.3. Typical oscillogram from the slip test	68
Fig. 4.4. Adjustable 3-phase reactor used as a load in the zero power-factor test	71
Fig. 4.5. Potier triangle method for the laboratory salient-pole synchronous generator ...	72
Fig. 4.6. Test set up for the sudden three-phase short-circuit test	75
Fig. 4.7. Typical short-circuit phase current waveform	76
Fig. 4.8. Currents oscillogram from sudden three-phase short-circuit test	80
Fig. 4.9. Phase-b short-circuit stator current alone with the dc field current	80
Fig. 4.10. Polynomial curve fitting of phase-b short-circuit current envelope	82
Fig. B.1. Typical oscillograms of sudden three-phase short-circuit at 0.6 pu rated voltage	97

List of Tables

Table 4.1 Test data from open- and short-circuit tests.....	64
Table 4.2 Experimental test result from the zero power-factor test.....	72
Table 4.3 Measured constants for the laboratory salient-pole synchronous generator.....	83
Table A.1 Typical constants of three-phase synchronous machines	95

List of Symbols

X_c	Characteristic reactance
ϕ	Magnetic flux
B	Magnetic flux density
H	Magnetic field intensity
N	Number of turns of an electric coil
l	The length of the magnetic path in metre
\mathcal{F}	Magnetomotive force
μ	Magnetic permeability in Henrys per metre
\mathcal{R}	Magnetic reluctance in Ampere-turns per Weber
v	The velocity in metre per second
λ	Flux linkage for a stator phase in (Weber-turns)
ω	The angular velocity of the rotor (rad/s)
r	Radius of the stator inner surface
e_a	Phase-a stator induced voltage
K_d	Distribution factor
K_p	Pitch factor
K_w	Winding factor
i_a, i_b, i_c	Stator phase currents
p	Number of poles for the machine

ω_s	Synchronous speed in (rad/s)
ω_m	Angular velocity in mechanical radians per second
n	Speed in revolutions per minute (rpm)
f	Electric frequency of the stator current in Hz
n_s	Synchronous speed in (rpm)
R_s	Stator winding resistance
X_l	Stator leakage reactance
X_{ar}	Armature reaction reactance
X_p	Potier reactance
E_g	Per-phase induced voltage in the stator winding
E_{ar}	Air-gap voltage
V_t	Terminal voltage of a synchronous generator
X_s	Synchronous reactance
L_s	Synchronous inductance
Z_s	Synchronous impedance
$V_{t(nl)}$	No-load terminal voltage
$V_{t(fl)}$	Full-load terminal voltage
K_m	Machine constant
\mathcal{F}_a	Armature (stator) mmf
\mathcal{F}_d	Direct axis component of armature mmf

F_q	Quadrature axis component of armature mmf
X_{ad}	Direct axis armature reaction reactance
X_{aq}	Quadrature axis armature reaction reactance
X_d	Steady-state direct axis synchronous reactance
X_q	Steady-state quadrature axis synchronous reactance
X'_d	Direct axis transient synchronous reactance
X''_d	Direct axis subtransient synchronous reactance
X'_q	Quadrature axis transient synchronous reactance
X''_q	Quadrature axis subtransient synchronous reactance
I_d	Direct axis component of stator current
I_q	Quadrature axis component of stator current
I_s	Steady-state component of stator current
I'	Transient component of short-circuit stator current
I''	Subtransient component of short-circuit stator current
T_a	Short-circuit armature time constant
T'_d	Direct-axis transient short-circuit time constant
T''_d	Direct-axis subtransient short-circuit time constant
δ	Power angle
θ	Power factor angle
Z_b	Base impedance

List of Abbreviations

AC	Alternating Current
DC	Direct Current
MVA	Megavolt-Ampere
IEEE	The Institute of Electrical and Electronics Engineers
AIEE	The American Institute of Electrical Engineers
IEC	The International Electrotechnical Commission
mmf	Magnetomotive force
emf	Electromotive force
BP	Blondel-Park
EBP	Extended Blondel-Park transformation
SSFR	Standstill Frequency Response Test
RSM	Rotary Synchronous Machine
LSM	Linear Synchronous Machine
FEM	Finite Element Method
AT	Ampere-Turns
Wb	Weber
VR	Voltage Regulation
PF	Power Factor
DQ	Direct and Quadrature

OCC	Open-Circuit Characteristic
SCC	Short-Circuit Characteristic
SCR	Short-Circuit Ratio
ZPFC	Zero Power-Factor Characteristic

Chapter 1

Introduction

1.1 General Background

In recent decades, synchronous generators, also called alternators, have become more and more a sustainable and principal source for the three-phase electric power. Synchronous generators of large power capacity (50MVA and above) normally have a high efficiency that can be greater than 98% [1]. The term synchronous stems from the fact that these machines, under steady-state operation, are precisely operated at a constant speed referred to as *synchronous speed*. They can mainly be classified into two different types; high-speed generators with a round or non-salient pole rotor structure and low-speed generators having a salient-pole rotor structure and relatively large number of poles. The former type is commonly known as a cylindrical rotor or turbo synchronous generator whereas the latter type is known as a salient-pole or hydroelectric synchronous generator. More details about the two generator types will be provided later in chapter 3.

For secure, reliable power delivery, a synchronous generator, whether it is operated alone to supply independent loads or interconnected with many others in large power grids, must be operated within certain operational limits (stability limits) that maintain its synchronism. Such operation modes are referred to as the *steady-state operation* of the synchronous generators. The analysis of synchronous machine performance under this condition can be made in a straightforward fashion. However, this is not always a trivial

task since abnormal conditions do take place frequently in typical power systems for a variety of causes. Therefore, it is crucial to predict and investigate the behaviour of synchronous machines during the abnormal or transient phenomena for better analysis and design results.

In a salient-pole generator, due to the non-uniform air gap geometry or rotor saliency, the air-gap inductances and thereby reactances will be time-varying with respect to the rotor angular position. This fact makes the analysis of such a generator a step more problematic than that of the cylindrical rotor synchronous generator where a uniform air-gap does exist. The synchronous reactance of a synchronous generator is defined as the algebraic sum of the leakage reactance of the stator winding and the magnetizing reactance due to the air-gap flux [2]. For a cylindrical rotor synchronous generator, synchronous reactance can be regarded as having one value at any instant of time. In contrast, the synchronous reactance can be resolved into two different components based on the two-axis theory proposed by Park [3] in the case of the salient-pole synchronous generator. Those components are commonly termed as direct-axis and quadrature-axis synchronous reactances as will be illustrated later on.

Synchronous reactance is one of the most significant parameters that affects and characterizes the performance of synchronous generators during various operational conditions. Its value is a function of the armature inductances and the angular frequency of the generated voltage. For a well-designed synchronous machine, synchronous reactance is supposed to have a small value to achieve high output power capability and thus high steady-state performance. However, as it plays a major role in eliminating the

large currents during transient conditions, a reduction of synchronous reactance should be limited to the machine's ability to overcome the transient state [4]. Knowing the cutting-edge methods to determine the various values of this reactance is therefore a very desirable objective for synchronous machines designers.

The focus of attention of this thesis is to find the direct-axis synchronous reactance values of a small practical salient-pole synchronous generator for various operation modes as well as the so-called *Potier triangle method*, which has been found to be a valuable means to compute the stator leakage reactance and armature reaction voltage drop of synchronous generators.

1.2 Literature Review

The following is a recent review of the previously done work about the studied topic. Much of the provided literature forms the major contributions of the IEEE and AIEE scholars and their associates to the art of synchronous machines analysis and design.

1.2.1 Historical Overview of the Two-Axis (dq-Axis) Theory

It is essential for synchronous machines analysis and design to develop a mathematical model that satisfactorily simulates their electric and mechanical behaviour during different operations and can be used with sufficient accuracy in various aspects. In general, most of the differential equations describing the electric and dynamic behaviour of a synchronous machine are highly nonlinear because of the existence of the time-varying inductances due to the rotor position. This fact often leads to more complexity in the analysis of those machines. A change of machine variables (flux linkages, currents

and voltages) has been found to be an effective way to reduce the complexity in the analysis of synchronous machines by eliminating the time-varying inductances from the voltage equations of the synchronous machine. This technique is referred to as *reference frame theory* [5].

In 1913, Andrew Blondel [6] in France suggested a new technique to facilitate the analysis of synchronous machines. This has been referred to as *Blondel two-reaction theory* ever since. The two-reaction theory [6] states that: "*When an alternator supplies a current dephased by an angle ψ with respect to the internal induced E.M.F, the armature reaction may be considered as the resultant of a direct reaction produced by the reactive current $I \sin\psi$ and a transverse reaction due to the active current $I \cos\psi$* ". In addition, it states that: "*The two reactions (direct and transverse) and the stray flux take place in three different magnetic paths: only the direct reaction acts in the main circuit of the field magnets, while the transverse reaction and the stray fields act, in general, upon circuits of low magnetic density*". To sum up, the principle behind Blondel's finding is to resolve the armature magnetomotive force (mmfs) and fluxes in a salient-pole synchronous machine into two different space components aligned with two orthogonal fictitious axes on the rotor [7]. Those axes are referred to as the direct-axis or d-axis, the magnetic axis of field winding, and the quadrature-axis or q-axis found in the interpolar space between salient poles and frequently assumed to lead the direct-axis by 90° .

Blondel's theory opened the door to several new research areas, especially in synchronous machines analysis and design. Consequently, a further exposition was presented in the USA by the AIEE members Doherty and Nickle [7] who tried to modify

the two-reaction theory and include some new considerations that Blondel did not account for in his fundamental proposition, such as the effect of mmf harmonics in both direct and quadrature axes.

Taking advantage of the work done by Blondel, Doherty and Nickle, R.H. Park [3] came up with a new means to analyze synchronous machines in the late 1920's. A traditional practice is to analyze three-phase synchronous machines in terms of phase variables (abc variables). However, Park made an attempt to simplify the analysis by proposing a certain mathematical transformation that tends to refer three-phase stator variables into new variables in a frame of reference fixed on a salient-pole rotor whose imaginary axes are the well-known direct- and quadrature- and zero-axis (dq0 coordinate system). Nowadays, this transformation is well recognized as Park's transformation, or the dq0 axis transformation. Under balanced three-phase conditions, Park's transformation can be regarded as a means of reducing three ac stator quantities into two dc quantities that are called dq-axis quantities, and the zero-axis quantities do disappear in such modes of operation [8, 9].

In 1933 [10], Park once again extended his previous contribution to the two-reaction theory to include the effect of the synchronizing and damping torque of a synchronous machine during the transients. Park's two-axis theory was further improved by Crary, Lewis and Zhang Liu and his associates [11, 12, 13]. In reference [11], Crary extended Park's previous work to include the effect of armature capacitance in the analysis of a salient-pole synchronous machine. He applied his new set of equations to solve problems involving the performance of a synchronous machine with capacitance circuits such as the

problem of self-excitation of a synchronous machine connected to a capacitance load or to a system through series capacitance. In reference [12], Lewis presented a new concept seeking to sweep away some further confusion that had been brought to attention due to Park's basic equations, such as having nonreciprocal mutual inductances in the derivation of an equivalent circuit and the use of per-unit system of notation. Basically, his work was devoted to the modification of the dq-axis equivalent circuit and corresponding equations previously obtained by R.H. Park and the others to be as straightforward and convenient as possible for further studies of synchronous machines.

Zhang Liu and his associates [13] proposed another extension of the Blondel-Park (BP) transformation that was referred to in their work as the EBP transformation. The new transformation is trying to not only consider the electric subsystem of the ac electric machines as Park's transformation does, but also to include the mechanical dynamics or the dynamics of the mechanical variables in the machine analysis.

Y.H. Ku [14] offered the rotating-field theory of ac rotating machines as a crucial alternative to the two-reaction theory in the electric machinery analysis. His analysis of synchronous machines included the hunting conditions besides the routine steady-state and transient analysis. He presented new components, called the forward and backward components, which are correlated to the familiar direct and quadrature components of the two-reaction theory. He showed how the new approach of analysis can form a basis of interconnection between synchronous and induction machines. More recently in 2004, an algebraic and geometric point of view of Park's transformation was presented by Emmanuel Del for a permanent magnet synchronous machine [15]. In general, Park's dq-

model and its numerous extensions have gained ground as a key tool in several computer representations and simulation studies on a wide variety of ac machinery ever since [8, 9, 16-25].

1.2.2 Determination of Synchronous Machine Parameters

The study of the behaviour of synchronous machines during steady-state and transient conditions requires an accurate knowledge of the equivalent circuit parameters of the machine. Synchronous machines are characterized by a number of constants, reactances and time constants. In particular, the direct-axis synchronous reactance is of tremendous importance as the capability chart, power transferred limitations and the short-circuit phenomenon of a synchronous machine are strictly defined by this parameter [26].

During the past several decades, many laboratory test procedures for practical determination of synchronous machine parameters have been initiated and documented in IEEE standard 115-1995 [27] and IEC standard 34-4 [28]. The standstill frequency response test (SSFR) [29-32] and the load rejection test [33, 34] have gained prominence due to their practically harmless effect on the tested machine and accuracy of the extracted test measurements. Standstill measurements have an advantage over the other testing methods, in that they can provide a significant amount of information about the tested machine. These are applicable to the d-axis and q-axis models and can provide a complete picture of both while most standard tests do not do so, especially with respect to the q-axis parameters [35].

The standstill frequency response test is performed by applying stator currents to the tested machine terminal at various levels of frequency, typically in a range from 0.001 Hz to 200 Hz. Thereafter, the machine parameters both in direct-axis and quadrature-axis can be evaluated by using the frequency response test data [36]. The load rejection test requires applying load rejection at two special operating points, in which the current components appear in the axis of interest only. At this point, for determination of direct-axis parameters, the tested machine, under-excited, has to be connected to a purely reactive power load to ensure that the fluxes and thus stator current components exist only in the direct-axis. In order to determine the quadrature-axis parameters, successive load rejection is needed to obtain a proper loading condition in such a way that only the q-axis component of the stator current is present. [34].

In 1918, R. E. Doherty and O. E. Shirley [37] developed a considerable refinement regarding the application of reactances in synchronous machines. They provided a broad study that provides several new fundamental concepts of armature reactance of synchronous machines. In addition, they presented a general formula for calculation of stator self-inductive reactance of synchronous machines and showed that the initial value of the short-circuit current of a synchronous machine is not only defined by stator self-induction, as is frequently assumed, but rather by a combination of both stator and field self-inductive reactances.

In [38], V. Karapetoff outlined the fact that the assumption of a constant armature leakage reactance in synchronous machines analysis may lead to wide deviation between the

computed and design data. Instead, he showed that the cyclic variation of the leakage reactance should be taken into account for higher accuracy levels in the analysis.

In 1928, R. H. Park and B. L. Robertson [39] gave a classification of the armature reactance in synchronous machines according to three categories: (1)- In terms of phase-sequence of stator current that can either be positive, negative or zero phase-sequence reactance. (2)- Methods of application in time of positive-sequence stator current that yields sustained, transient and sub-transient reactance. (3)- In the position of the rotor that gives rise to direct-axis and quadrature-axis reactance. Stator reactance due to the armature reaction and the stator leakage reactance are combined in one quantity that is commonly known as the synchronous reactance.

The three-phase short-circuit test has been recognized as a vital test procedure to study transient characteristics of synchronous generators. The test is made to determine test values for specified machine parameters, thus reactances and time constants, of synchronous generators. Briefly, the sudden three-phase short-circuit test can be carried out by developing a symmetrical three-phase short-circuit at the terminals of the tested generator when it is operated at rated speed and at various percentages of the rated terminal voltage. The most usual practice has been to perform the test at a no-load condition. Nevertheless, it can be made under various loading conditions. An oscillogram of the instantaneous stator phase currents following the short circuit can then be recorded and analyzed by an appropriate method of analysis to extract the relevant subtransient and transient machine reactances and time constants [40].

A discussion about the three-phase short-circuit method is given for both no-load and load cases, for both a cylindrical rotor and salient-pole synchronous machine, by R. E. Doherty and C. A. Nickle in [41]. The effect of stator resistance on short-circuit currents is illustrated by two cases: resistance is at first negligible and then it is considered. Also, the effect of the load's nature on the short-circuit current is absorbed. The investigations showed that short circuits under load may generate less current than those applied at no-load. It has also been shown that the second harmonic components in the short-circuit current depend on the difference between the sub-transient direct-axis and quadrature-axis reactances and may be eliminated by proper damper windings.

Primary concepts and practical considerations of test methods to compute synchronous machine parameters are discussed by Sherwin H. Wright in [42]. Test procedures to obtain the most important machine constants, the machine reactances, resistance and time constants, are illustrated and tabulated test results are given. Tests included the three-phase short-circuit test and slip test.

L. A. March and S. B. Cray [43] discussed the determination of armature leakage reactance using the so-called *Potier method*. They showed how Potier reactance varies with the increase in the field current for a salient-pole machine and how it can practically be a constant value for a synchronous machine with a cylindrical rotor. They mentioned that the Potier reactance when measured at rated terminal voltage could be much greater than the actual armature leakage reactance for a synchronous machine. Alternatively, they suggested that the Potier reactance when measured at a higher value of terminal voltage and thus a higher field current can result in a more accurate approximation of the

armature leakage reactance than the classical measuring at normal voltage. However, this approach has been found to be somewhat risky as the machine under test may not tolerate the increased high values of field current at which the determination of armature leakage reactance by the Potier method can be accurate. As a consequence, A. M. El-Serafi and J. Wu [44] proposed an alternative testing method to accurately determine the armature leakage reactance that can be applied without any risk to the tested machine, unlike the preceding approach in [43]. In the proposed method, the curve of the terminal voltage/armature current characteristic with the machine unloaded and unexcited is required along with the open circuit characteristic.

Canay has contributed significantly to the art of determination of synchronous machine parameters with a series of important papers [45-48]. He obviously focused his attention to more correct determinations of rotor circuit parameters. Throughout his investigation, Canay showed how one would make an accurate estimation of the synchronous machine equivalent circuit parameters without making the usual simplifying assumptions or iterations that can be a source of wide discrepancies in the results of the analysis.

It has been realized that the conventional equivalent circuit diagram found in the earlier theory of the synchronous machine does accurately represent the stator circuit only. However, Canay revealed that transients for rotor quantities (i.e. field current, field voltage, etc.) can also be specified if a suitable equivalent circuit diagram that represents both the stator and rotor circuits is used. For this purpose, he employed a new reactance, termed as *the characteristic reactance* X_c to be used instead of the traditional stator leakage reactance in the newly developed equivalent circuit diagram of a synchronous

machine. The characteristic reactance X_c is independent of rotor reference quantities and can be found directly from the measurement of the alternating current transfer between stator and field windings. This can easily be done by measuring field current variations during a sudden three-phase short-circuit test. In general, X_c for turbomachines is greater than the stator leakage reactance whereas it is much lower than the stator leakage reactance for a salient-pole synchronous machine. It is noteworthy that, unlike the generalized Parks' dq-axis model which has only two rotor circuits (one field winding and one damper winding), Canay's model can be valid for higher order machine models with more than two rotor circuits in both direct-axis and quadrature-axis [49].

In [50], L. Salvatore and M. Savino attempted to remove some simplifying assumptions that have been set forth in the traditional analysis of synchronous machines and which resulted in inaccurate determination of the machine parameters. They used a model of analysis with two windings (field and damper) in the direct-axis circuit. Then, they examined their model with two standard tests; the sudden three-phase short circuit and stator decrement test with short-circuited field windings. They demonstrated that it is possible to determine the model parameters in terms of a set of measurable time constants regardless of whether equal or unequal direct-axis mutual reactance between the stator, field and damper windings was assumed.

A general survey of methods for determination of machine parameters of the electric equivalent circuit of rotary synchronous machines (RSM) is conducted in [51]. It gives an overview of the most used testing methods for determination of synchronous machine parameters that are defined in IEEE standards 115 and 115-A, besides some other

traditional testing methods. Thereafter, the paper uses the reviewed methods to propose analogous techniques for estimating machine parameters for linear synchronous machines (LSM).

Determination of synchronous machine parameters using network synthesis techniques is given in reference [49]. The paper used a d-axis model that contains more than one damper winding that is based on the direct-axis equivalent circuit of Canay's generalized model of synchronous machines to prove that no unique direct-axis circuit can be determined from two-port information. Also, shown in the paper is the noteworthy observation that only limited d-axis parameters can be found in a unique way for a synchronous machine model with more than one damper winding in the rotor circuit.

In [52], the authors proposed a new estimation procedure for determination of direct-axis parameters of a synchronous machine. In this method, all the parameters derivation was done using the Matlab derivation program. For more accurate results, a gradient-based optimisation algorithm was also employed to adjust the machine parameters so that a close agreement between the simulated terminal voltage response and the measured voltage response could be reached. A better determination of synchronous machine parameters was also presented by a group of IEEE authors [36]. They suggested a simple and accurate approach to estimate the direct-axis and quadrature-axis stator inductances of a synchronous machine by applying a hysteresis based current control of the direct and quadrature components of stator current.

In recent times, the finite element method (FEM) is found to be a valuable means for estimating most synchronous machine parameters due to its advantages over the classical testing methods in its ability to consider more important factors and avoid many hypotheses by the analysis of the electromagnetic field in the machine's iron core [53-56].

1.3 Thesis Objectives

The major contribution of this research work is to determine the steady-state, transient, and subtransient values of the direct-axis synchronous reactance of a practical salient-pole synchronous generator. Moreover, the *Potier triangle method* is developed and presented for a laboratory salient-pole synchronous generator in this thesis. This method makes it possible to compute the Potier reactance, the drop in the terminal voltage due to armature reaction and the required excitation corresponding to the rated voltage for any specified load current of a synchronous generator. For those objectives, certain standard tests corresponding to the IEEE standard 115-1995 [27] are carried out on the studied generator, among them the implementation of the well-recognized sudden three-phase short-circuit test.

1.4 Outline of the Thesis

This thesis is broken down into five chapters that can be stated as follows:

Chapter 1 provides a general introduction and a recent review of the previous literature related to the scope of the thesis.

Chapter 2 describes the fundamental concepts of rotating electric machines.

Chapter 3 gives a full explanation about the theory of synchronous generators within the scope of this thesis.

Chapter 4 provides the experimental test results that were obtained in the laboratory by performing specific standard tests on the considered synchronous generator.

Chapter 5 is the conclusion and recommendations of the work that may be done in the foreseeable future regarding the selected research topic.

Chapter 2

Rotating AC Machinery Fundamentals

The rotating ac electric machines can mainly be divided into two types: synchronous machines and induction machines. These machines are widely used in the industry for both generator and motor applications. As its name implies, the rotating machinery principle is based on the production of the rotating magnetic field inside the machine. The object of this chapter is to provide an essential description of the fundamental concepts of the rotating machines.

2.1 Basics of Magnetic Circuits

It is of utmost importance in electric machinery design and analysis to have a basic knowledge of magnetic circuits. The principle of such circuits is in fact similar to that of electric circuits. An electric circuit provides a path for the electric current to flow through. Similarly, a magnetic circuit yields a closed path to flow for the magnetic flux traveling through it. The electric current flowing in an electric circuit is generated by the voltage source or the electromotive force (emf) of that circuit. By analogy, the magnetomotive force (mmf) is responsible for establishing the magnetic flux in a magnetic circuit. For proceeding with this discussion, let us refer to the magnetic circuit in Fig.2.1.

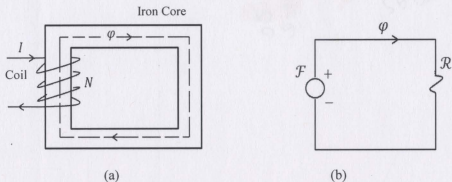


Fig.2.1 (a) Typical magnetic circuit elements, (b) Equivalent circuit diagram

Fig.2.1 shows a simple magnetic circuit with its equivalent circuit. It can be noted that this is basically identical to the transformer configuration except for the absence of the secondary winding. As a current (I) flows through a coil of (N) turns around the iron core, a significant amount of the net flux established by this current will be confined by the iron core due to the very high permeability of the iron. There is still a small portion of the flux that spreads out in the air around the iron core. This flux is commonly known as the leakage flux. The leakage flux might have a noticeable impact on the performance of such electromagnetic devices.

The magnetic flux density is defined as the ratio of the total flux (ϕ) to the area (A) of the ferromagnetic material in which the flux is confined. Thus, ϕ

$$B = \frac{\phi}{A} \quad \text{Weber per square meter (Wb/m}^2\text{)} \quad (2.1)$$

The unit (Wb/m^2) is now denoted by the IEEE standard symbol (T) or Tesla.

The magnetomotive force (mmf), denoted by (\mathcal{F}), in a current-carrying conductor is equal to the product of the current in the electrical conductor times the number of its turns. Thus

$$\text{mmf} = \mathcal{F} = N \times I \quad \text{Ampere-Turns (AT)} \quad (2.2)$$

In terms of the magnetic field intensity (H), the above equation can be rewritten as:

$$\mathcal{F} = H \times l \quad (2.3)$$

where H is measured in ampere-turns per metre (AT/m).

l is the length of the magnetic path in metre.

It is evident from Fig.2.1 (b) that there is an analogy between electric and magnetic circuits regardless of the difference in the nature of their parameters. The magnetomotive force, mmf, can now be expressed in terms of the equivalent magnetic circuit parameters as follows:

$$\mathcal{F} = \mathcal{R}\varphi \quad (2.4)$$

where φ is the flux in Weber (Wb).

\mathcal{R} is called the reluctance of the magnetic circuit that corresponds to the resistance in an electric circuit. The reluctance is generally defined by the following relationship:

$$\mathcal{R} = \frac{l}{\mu A} \quad \text{Ampere-turns per Weber (AT/Wb)} \quad (2.5)$$

where,

l : The length of the closed magnetic path (m).

A: The cross-sectional area of the magnetic material (m^2).

μ : The permeability of the magnetic material in Henrys per metre (H/m).

2.2 Induced Voltage Equation

If a current-carrying conductor of length (l) moves in a magnetic flux area of density B , the conductor will then experience a force (F) that tends to rotate it. The direction of the rotation is given by Fleming's left-hand rule [57]. This is actually the basis of a *motor action* electric machine. With this in mind, it can be written:

$$F = B \times l \times i \quad (\text{N}) \quad (2.6)$$

where (i) is the current through the conductor in Amps.

In contrast, the basic principle of an electric generator is based on the *flux-cutting* action of Faraday's law, which states that whenever a conductor cuts constant magnetic field lines, a voltage will be induced across the conductor terminals. The voltage will also be induced if the flux is time-varying while the conductor is held stationary. The polarity of this voltage is determined by the right-hand rule of Fleming. The induced or generated voltage is referred to as the counter emf for the motor case. The induced voltage is thus defined as:

$$emf = B \times l \times v \quad (\text{Volt}) \quad (2.7)$$

where B , v and l are mutually perpendicular [58].

B : The flux density of the magnetic field in Tesla.

v : The velocity by which the conductor crosses the flux lines in (m/s).

l : The length of the conductor in metre.

Generally, if the conductor moves at an angle (θ°) with respect to the flux lines as seen in Fig.2.2, the induced voltage equation will then be:

$$emf = B \times v \times l \times \sin(\theta) \quad (\text{Volt}) \quad (2.8)$$

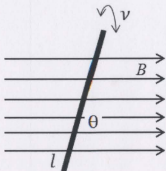


Fig.2.2 A conductor moving with an angle (θ°) through a magnetic field [57]

This is only the emf induced in a single wire; let us now find the expression of the equation governing the induced emf in a set of three-phase windings such as those accommodated by the stator of synchronous and 3-phase induction machines.

In the three-phase rotating machines, three-phase windings are placed on the stator 120 electrical degrees apart in the space from each other in order to produce as sinusoidal as possible induced voltage. Consequently, the induced voltages in the stator windings have an equal magnitude and they are 120° out of phase from each other. Fig.2.3 shows a cross-sectional view of a typical 2-pole 3-phase ac machine. The rotor poles are assumed to spin at an angle (θ°) with respect to the phase a stator winding.

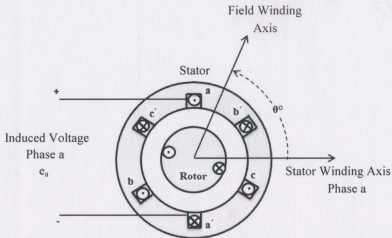


Fig.2.3 Schematic diagram of a 2-pole 3-phase ac machine [58]

The flux density wave distributing in the air-gap of the machine is assumed sinusoidal in space and therefore defined as follows:

$$B = B_m \cos \theta \quad (2.9)$$

Thus, it has a maximum value (B_m) at $\theta = 0$, and it decays to zero at $\theta = 90^\circ$

The air-gap flux per pole can be obtained by the linear integral of the flux density over the area covered by one pole ($\theta = \pi$ radians). Thus,

$$\varphi = \int_{-\pi/2}^{+\pi/2} B_m \cos \theta \, l r \, d\theta = 2 B_m l r \quad (2.10)$$

where (l) is the axial length of the stator, (r) is the radius of the stator inner surface.

The above equation computes the per pole flux for a two-pole ac machine. More generally, for a machine with p -number of poles, the flux equation can be rewritten as:

$$\varphi = \frac{4}{p} B_m l r \quad (2.11)$$

In accordance with Faraday's law, the induced emf in one phase of the stator windings can be expressed as follows:

$$e = -\frac{d\lambda}{dt} = -N \frac{d\varphi}{dt} \quad (\text{Volts}) \quad (2.12)$$

where λ is the flux linkage for a stator phase in (Weber-turns) and is equal to

$$\lambda = N \varphi \cos \omega t \quad (2.13)$$

where $\omega = 2\pi f$ is the angular velocity of the rotor (rad/s), N : number of turns per stator phase.

The phase-a induced voltage (emf) is thus:

$$e_a = \omega N \varphi \sin \omega t = 2\pi f N \varphi \sin \omega t \quad (2.14)$$

from which the maximum value of the induced voltage per phase is

$$E_m = 2\pi f N \varphi \quad (2.15)$$

Therefore, the rms per phase induced voltage is

$$E_{rms} = \frac{E_m}{\sqrt{2}} = 4.44 f N \varphi \quad (2.16)$$

In a practical ac machine, the armature windings on the stator are often distributed in slots and made short-pitch to improve the sinusoidal shape of the induced voltage. Therefore, the distribution and pitch factors denoted by K_d and K_p , respectively must be taken into account. Hence, we have:

$$E_{rms} (\text{per phase}) = 4.44 N f \phi K_d K_p = 4.44 N f \phi K_w \quad (2.17)$$

K_w is known as the winding factor for the stator distributed windings which equals the value of $(K_d K_p)$ and falls in the range of $(0.85 - 0.95)$ [59].

Eventually, the three-phase set of the induced voltage can be expressed as:

$$e_a = E_m \sin \omega t \quad (2.18)$$

$$e_b = E_m \sin (\omega t - 120^\circ) \quad (2.19)$$

$$e_c = E_m \sin (\omega t + 120^\circ) \quad (2.20)$$

2.3 Rotating Magnetic Field in AC Machinery

As pointed out earlier, in ac machines, a three-phase voltage can be induced by means of flux-cutting action or the presence of the magnetic field in the machine air-gap. Similarly, a balanced three-phase set of currents can produce a rotating magnetic field when flowing through a set of three-phase windings. Hence, the revolving magnetic field is created by the stator supply current in a motor action ac machine, whereas it is established by the load current in a generator action ac machine. Knowing the nature of the waveform of this magnetic field is an important aspect of understanding the behaviour of ac machinery. In rotating ac machines, such as three-phase synchronous and induction machines, three-phase windings, each 120 electrical degrees apart, are placed on the stator as shown in Fig.2.5(a). These windings are commonly distributed in the stator slots. A balanced three-phase current is then applied to the stator distributed windings so that a revolving magnetic field is established in the air-gap. It is actually the sinusoidally distributed mmf

induced in the stator windings that is the source whereby the rotating magnetic field is created. Its amplitude and direction depend on the instantaneous current in each phase of the stator windings. The currents' reference directions are indicated by dots and crosses in Fig.2.5(a). The balanced three-phase stator current, as shown in Fig.2.4, may be defined as follows:

$$i_a = I_m \cos \omega t \quad (2.21)$$

$$i_b = I_m \cos(\omega t - 120^\circ) \quad (2.22)$$

$$i_c = I_m \cos(\omega t + 120^\circ) \quad (2.23)$$

Each of these currents will produce a sinusoidally distributed mmf wave in the individual phase winding through which it is flowing. Therefore, the resultant mmf distributing in the air-gap of the machine is the sum of the three mmf waves from each phase winding alone as seen in Fig.2.5(b). Since the applied three-phase currents are balanced and the stator windings are shifted by 120° in the space from each other, the three components of the resultant mmf wave also have a 120° displacement in time from each other.

❖ Graphical Approach of the Distributed Stator MMF Wave

Let us now investigate the amplitude of the travelling mmf wave in ac machines. From Fig.2.4, at instant of time ($\omega t = 0^\circ$), the phase a current is at its maximum value. As a result, the mmf wave of phase a, represented by the vector (F_a) in Fig.2.5, also has its maximum value ($F_{\max} = NI_m$) and is aligned with the magnetic axis of phase a. At the same

moment, the corresponding mmf waves of the other two phases have equal magnitude which can be expressed as follows [59]:

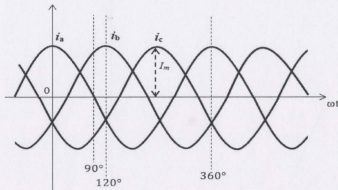


Fig.2.4 Balanced 3-phase current applied to the stator of ac machine

$$F_b = F_c = -\frac{F_{\max}}{2} \quad (2.24)$$

The resultant stator mmf (F_T) can now be found by the vector sum of its three components as seen in Fig. 2.6 (a) as:

$$F_T = F_a + F_b + F_c \quad (2.25)$$

$$F_T = F_{\max} + \frac{F_{\max}}{2} \cos 60^\circ + \frac{F_{\max}}{2} \cos 60^\circ = \frac{3}{2} F_{\max} = \frac{3}{2} N I_m \quad (2.26)$$

where N is the number of turns per stator phase.

I_m : the maximum value of the phase current.

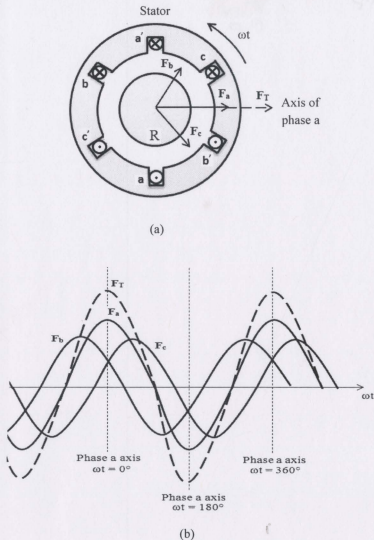


Fig.2.5 Production of the armature (stator) mmf wave in ac rotating machines; (a) Cross-sectional view of 2-pole ac machine, (field windings are not shown) [58], (b)The resultant stator mmf wave with its components [59]

It is obvious from Eq. (2.26) that the net mmf wave is a sinusoidally distributed wave moving in the positive direction along the magnetic axis of phase a with an amplitude equal to $(3/2)$ times the amplitude of the phase a mmf wave alone.

At a later time ($\omega t = 90^\circ$), the instantaneous value of the phase currents are

$$i_a = 0 \quad i_b = \frac{\sqrt{3}}{2} I_m \quad i_c = -\frac{\sqrt{3}}{2} I_m \quad (2.27)$$

Therefore,

$$F_a = 0 \quad F_b = \frac{\sqrt{3}}{2} F_{\max} \quad F_c = -\frac{\sqrt{3}}{2} F_{\max} \quad (2.28)$$

Similarly, the total mmf wave is the vector sum of the three components as in Fig. 2.6 (b).

$$F_T = 0 + \frac{\sqrt{3}}{2} F_{\max} \cos 30^\circ + \frac{\sqrt{3}}{2} F_{\max} \cos 30^\circ = \frac{3}{2} F_{\max} = \frac{3}{2} N I_m \quad (2.29)$$

Again, the resultant mmf wave has the same amplitude and sinusoidal waveform as those found in the preceding instant.

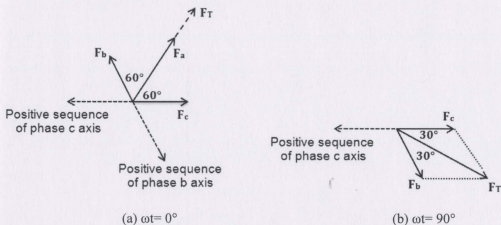


Fig.2.6 Vector diagram of the resultant mmf wave [57]

Another example demonstrating this fact is the instant of time ($\omega t = 120^\circ$) when phase b current has its positive peak value as illustrated in Fig.2.4. The instantaneous value of the phase currents and the associated mmf components are now as follows:

$$i_a = -\frac{1}{2} I_m \quad F_a = -\frac{F_{\max}}{2} \quad (2.30)$$

$$i_b = I_m \quad F_b = F_{\max} \quad (2.31)$$

$$i_c = -\frac{1}{2} I_m \quad F_c = -\frac{F_{\max}}{2} \quad (2.32)$$

The resultant mmf wave (F_T) is

$$F_T = \frac{F_{\max}}{2} \cos 60^\circ + F_{\max} + \frac{F_{\max}}{2} \cos 60^\circ = \frac{3}{2} F_{\max} = \frac{3}{2} N I_m \quad (2.33)$$

Thus, the resultant mmf wave is once again sinusoidally distributed having the same amplitude, but this time is centred on the magnetic axis of the phase b winding.

It can clearly be seen that as time passes, the resultant mmf wave distributing in the air-gap of an ac machine retains its sinusoidal form with a constant amplitude of $(\frac{3}{2} F_{\max})$, where F_{\max} is the maximum value of the mmf wave produced by any individual phase winding. It is also moving around the air-gap at a constant angular velocity $\omega_s = 2\pi f$ (rad/s).

In general, for a p -pole machine, the mechanical speed of rotation for the travelling mmf wave is:

$$\omega_m = \frac{2}{p} \omega_s = \frac{4\pi f}{p} \quad (\text{rad/s}) \quad (2.34)$$

or

$$n = \frac{120 f}{p} \quad (\text{rpm}) \quad (2.35)$$

where

f is the electric frequency of the stator current in Hz.

p is the number of poles for the machine.

ω_m is the angular velocity in mechanical radians per second.

n is the speed in revolutions per minute (rpm).

In fact, in the synchronous machine theory, the speed at which the rotating magnetic field rotates in the air-gap is precisely equal to the rotor speed and is referred to as *the synchronous speed* (n_s).

Chapter 3

Analysis of the Synchronous Generator

Over the years, synchronous generators, also called alternators, have been used as a reliable ac electric power source. Therefore, it is of great importance to have a basic knowledge of this kind of ac machinery, its construction, principles of operation and performance characteristics. For this object, this chapter is developed. The focus of attention will particularly be the salient-pole synchronous generator since it represents the machine being dealt with in this thesis.

3.1 Brief Overview

A synchronous generator is a three-phase ac electric machine that converts mechanical input power into electric output power and rotates at a constant speed referred to as the *synchronous speed*. The word 'synchronous' comes from the fact that in this kind of ac machine, the rotor and its associated dc magnetic field must have precisely the same speed as the rotating magnetic field produced by the stator currents. Thus, the rotor speed is a function of the number of poles of the machine and the electric frequency (Hz) of the stator current. Synchronous generators operate a large number of various loads with wide rating ranges. They have been extensively studied and examined in the literatures. Synchronous generators, based on their speed of rotation, can be divided into two categories: high-speed and low-speed generators. The high speed generators are often

driven by means of steam or gas turbines. They are known as turbo or turbine-generators. The low speed generators, on the other hand, are driven by means of waterwheel (hydraulic) turbines. Hence, they are named hydro-turbine or water-wheel synchronous generators. The actual distinction between the two types of synchronous generators lies in the rotor structure, as will be clarified later in this chapter.

3.2 Physical Construction

A typical synchronous generator consists of the following essential elements:

3.2.1 The Stator

The stator of a synchronous generator is identical to that for an induction machine. It is built of thin iron laminations of highly permeable steel core. The laminated core is to reduce the magnetizing losses such as the eddy current and hysteresis losses. The stator accommodates the three-phase armature windings which are the distributed stator windings. The distributed windings are embedded in the slots inside the stator core 120 electrical degrees apart in the space to minimize the space harmonics in the resultant air-gap flux waveform. They are also made short-pitch in order to produce a smooth sinusoidal voltage waveform at the stator terminals. The reason behind having the armature windings fixed on the stator is that they need to be well-insulated due to the high voltages and transient currents they may experience during different operation modes. A cross-sectional sketch of a stator of a synchronous machine is shown below in Fig.3.1

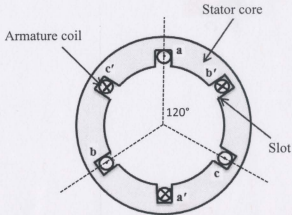


Fig.3.1 Basic Stator Scheme for a 2-pole 3-phase synchronous generator

3.2.2 The Rotor

The rotor of the synchronous generator hosts windings which carry the dc field current and are connected to the excitation source of the generator via brushes and the slip rings assembly. The synchronous generator has two different rotor configurations based on its speed. Turbo-generators used for high speed operation have a round rotor structure. These generators are commonly referred to as non-salient pole or cylindrical-rotor synchronous generators. They have a uniform air-gap and normally have either two or four field poles, depending on the required speed of operation. Hydro-generators used for low speed operation have rotors with salient poles structure. These generators are known as salient-pole synchronous generators. Because of the rotor saliency, a non-uniform air-gap is formed between the rotor and stator inner surface. The salient-pole rotor has a comparatively larger number of poles. A common practice is to have *damper* or *amortisseur* windings equipped to the rotor of this type in order to damp out the speed oscillation in the rotor. Damper windings are copper or brass bars embedded in the salient

pole faces with both their ends shorted-circuited by means of shorting rings to form a cage structure similar to that for a squirrel cage rotor of an induction machine. These windings play a major role in retaining the generator synchronism during the *dynamic transient* or *hunting*. The cross-sectional view of two rotor structures of the synchronous generator are shown in Fig.3.2

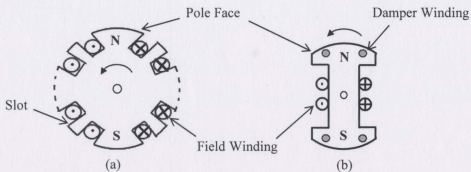


Fig.3.2 Elementary rotor structure of 2-pole alternator: (a) cylindrical rotor, (b) salient-pole rotor [60]

3.3 Principle of Operation

The field winding on the rotor of a synchronous generator is supplied by dc field current from an external dc source which is called the exciter for the generator. Based on the exciter arrangement, use of slip rings may or may not be needed for this purpose. The field current will then produce a constant magnetic flux around the rotor in the air-gap. The rotor is rotated by means of a prime mover at the synchronous speed (n_s) of the generator. As a result, a set of balanced three-phase voltages will be induced in the distributed stator (armature) windings in the stator due to the flux-cutting action or Faraday's law. If a load is connected to the generator terminals, a time-varying current

will flow through the three-phase stator windings causing a synchronously revolving magnetic field to be established in the air-gap. For maintaining the synchronism, the rotating magnetic field must be locked in or synchronized with the mechanical constant speed of the rotor magnetic field. In other words, the revolving magnetic field produced by the stator rotates at the same synchronous speed as the rotor and is therefore stationary with respect to it. The synchronous speed can be defined by the following relationship:

$$n_s = \frac{120 f}{p} \quad (\text{rpm}) \quad (3.1)$$

OR

$$\omega_s = \frac{4\pi f}{p} \quad (\text{rad/s}) \quad (3.2)$$

where

f is the stator electric frequency in Hz.

p is the number of poles for the machine.

ω_s is the synchronous speed in radians per second.

n_s is the synchronous speed in rpm.

3.4. Equivalent Circuit of Synchronous Generator

As pointed out earlier, the stator of a synchronous generator has three-phase armature windings distributed inside the slots of its core. These stator windings can be either Y- or Δ -connected. However, they are often connected in Y-form for convenience. Fig.3.3 indicates the typical Y-connected stator windings with their parameters. The stator windings have a resistance (R_s) and reactance due to the leakage flux linking the winding

called leakage reactance of the stator winding ($X_l = 2\pi f L$), where L is the leakage inductance of the armature winding in Henry. The armature resistance is very small compared to the armature leakage reactance and may thus be neglected.

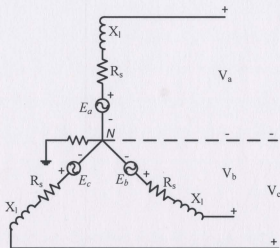


Fig.3.3 Y-connected 3-phase stator distributed windings of a synchronous machine

The value of the per phase stator resistance (R_s) can easily be found by a simple dc measurement of the resistance between any two phases at a time. The line-to-line average dc resistance (R_{dc}) is obtained. For Y-connected stator windings, the per phase effective (ac) stator resistance is then equal to:

$$R_s = \frac{1}{2} K R_{dc(L-L)} \quad \Omega \quad (3.3)$$

where K is a factor which rises due to the skin effect caused by the alternating (ac) stator current and is approximated to be 1.6 for 60 Hz operation [59]. The thermal effect of the stator current is also included in this factor.

3.4.1 Armature Reaction

The load current when flowing in the stator windings of a synchronous generator produces its own magnetic field. This magnetic field will distort the main air-gap flux set up by the rotor field winding. In other respects, the magnetic field due to the load current is said to be either demagnetizing or magnetizing the original air-gap flux depending on the power factor of the load. The magnetizing effect of the armature or stator flux on the air-gap flux is referred to as the *armature reaction*. The effect of the armature reaction in synchronous generators is taken into consideration by assigning to it a corresponding fictitious reactance called armature reaction reactance or simply the magnetizing reactance (X_{ar}).

3.4.2 Equivalent Circuit Representation Including Armature Reaction

For the sake of deriving the steady state machine equations for the synchronous generator, a proper equivalent circuit should be developed. Fig.3.4(a) shows the per-phase equivalent circuit of a synchronous generator in terms of the armature reaction reactance (X_{ar}) and the armature leakage reactance (X_l).

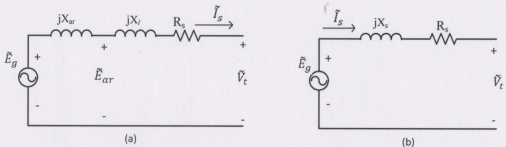


Fig.3.4 Single-phase equivalent circuit of a cylindrical rotor synchronous generator: (a) including armature reaction effect, (b) comprising the synchronous reactance

Note that this representation only includes the stator circuit. Since it carries the dc field current, the rotor circuit may however be modeled simply by a single coil of (N_f) turns connected to a dc voltage source (V_f) .

In Fig.3.4; \vec{I}_s is the phasor stator current per phase.

\vec{E}_g : is the per phase induced voltage

\vec{V}_t : is the per phase terminal voltage

\vec{E}_{ar} is called the *air-gap voltage* or the *voltage behind the armature leakage reactance*. It is induced to account for the resultant air-gap flux [58].

The reactance due to the armature reaction X_{ar} and armature leakage reactance X_l are normally combined in one reactance known as *synchronous reactance* X_s . Hence,

$$X_s = X_{ar} + X_l \quad (3.4)$$

The synchronous reactance can also be expressed in terms of the synchronous inductance L_s as:

$$X_s = 2\pi f L_s \quad (3.5)$$

The synchronous inductance (L_s) is defined as the effective inductance as viewed from the armature windings under steady-state operation. Neglecting the effects of saliency, as with the cylindrical rotor synchronous machine, the synchronous inductance and thereby the reactance of the armature winding are independent of the rotor position (θ_m). Thus, they can be assumed as a constant [58].

The synchronous impedance is defined as

$$\tilde{Z}_s = R_s + j X_s \quad (3.6)$$

R_s is often omitted for its relatively very small value for large synchronous machine analysis.

The per-phase equivalent circuit comprising the synchronous reactance of the stator windings in series with the stator resistance is shown in Fig.3.4 (b). Note that this model is essentially employed for a cylindrical rotor (non-salient pole) synchronous generator. For a salient-pole synchronous generator, the synchronous reactance has two different components perpendicular to each other as will be seen later in this chapter.

Using the developed equivalent circuit, let us now find the expression of the air-gap induced voltage. This can be stated as:

$$\tilde{E}_g = \tilde{V}_t + \tilde{I}_s R_s + \tilde{I}_s j(X_{ar} + X_l) \quad (3.7)$$

or

$$\tilde{E}_g = \tilde{V}_t + \tilde{I}_s R_s + j\tilde{I}_s X_s = \tilde{V}_t + \tilde{I}_s \tilde{Z}_s \quad (3.8)$$

where the script (\sim) denotes the phasor form of the associated quantities.

The change in the terminal voltage magnitude from the no-load to full-load operation of a synchronous generator with constant speed and excitation is visualized by a percentage value known as the *voltage regulation*, $VR(\%)$. The expression of voltage regulation is given as follows:

$$VR(\%) = \frac{(V_{t(nl)} - V_{t(fl)})}{V_{t(fl)}} \times 100\% \quad (3.9)$$

where

$V_{t(nl)}$ is the no-load terminal voltage (equals the induced voltage E_g)

$V_{t(fl)}$ is the full-load terminal voltage.

The voltage regulation (VR%) may be a negative or positive value based on the nature of the load current. For a synchronous machine operating as a generator, the percentage voltage regulation is normally a large positive value for a lagging load, a small positive value for a unity power factor load and a negative value for a leading power factor load. The reasons behind that will be explained in the next section.

3.5 Effect of Load Changes on the Excitation

At no-load operation, the terminal voltage of a synchronous generator is equal to the induced voltage because there will be no voltage drop in the armature windings. However, for a loaded generator, due to the armature reaction associated with the load current, there will be either a reduction or increase in the terminal voltage. Fig.3.5 shows the phasor diagram of a cylindrical rotor synchronous generator with various loads (lagging, unity and leading PF).

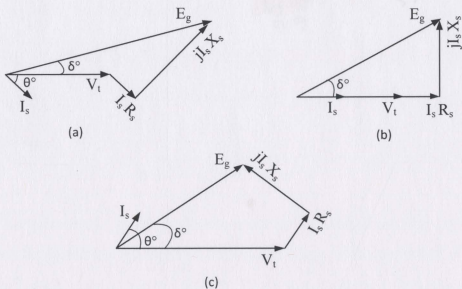


Fig.3.5 Phasor diagram of a cylindrical rotor synchronous generator: (a) lagging power factor load, (b) unity power factor load, (c) leading power factor load [61]

In the above phasor diagram, the angle (δ°) between the induced voltage and terminal voltage is referred to as the *torque or power angle*. The angle (θ°) between the load current and the terminal voltage is the power factor (PF) angle of the load.

To restore the terminal voltage of a loaded synchronous generator to its rated value, a course of action must be taken. Thus, the induced voltage must be changed in correspondence with the variations in the terminal voltage to overcome the armature reaction voltage drop. Referring to Eq. (2.17) in chapter 2, the rms per-phase induced voltage can simply be rewritten as:

$$E_{rms} = K_m \phi \omega \quad (3.10)$$

where

K_m is known as machine constant, ϕ is the flux per stator pole in (Weber).

$\omega = 2\pi f$ is the angular speed of the rotor (electrical rad/s)

It is evident that the induced voltage is proportional to the resultant flux in the machine and speed of operation. The induced voltage can thereby be changed either by controlling the flux or the speed of rotation of the generator. The speed must be held constant for a constant frequency operation. The induced voltage may then be changed by varying the net flux in the air-gap. This can be made achievable by a proper adjustment to the dc field current fed into the rotor winding. This approach to maintain the terminal voltage at the desired level is known as excitation control of the synchronous generator. This discussion may be illustrated by the following three cases:

3.5.1 Lagging Power Factor Load

It can be seen from Fig.3.5(a) that for a lagging PF load (inductive load), the terminal voltage will be reduced. Therefore, the induced voltage must be increased to keep the rated terminal voltage. The reason for this reduction in the terminal voltage is that the armature reaction due to the lagging load current is said to be demagnetizing or weakening the air-gap flux. As a result, a large amount of excitation (over-excitation) is needed to overcome the air-gap flux demagnetization. If more loads are now added to the generator at the same PF, then the armature voltage drop $I_a X_s$ will be even greater, causing a significant reduction in the terminal voltage. In this respect, the voltage regulation has a large positive value for a synchronous generator with a lagging PF load.

3.5.2 Unity Power Factor Load

In the case of unity power factor loads (zero reactive power), Fig.3.5(b), there will be a slight reduction in the terminal voltage due to the armature reaction effect of the unity PF load current. Therefore, the induced voltage of the generator should also be increased to retain the rated terminal voltage. In fact, the increase in the induced voltage needed here is less than that for the lagging PF case. As a result, the voltage regulation under such an operation mode is a small positive value [61].

3.5.3 Leading Power Factor Load

From the phasor diagram in Fig.3.5(c), it can be observed that the terminal voltage can be greater than the induced voltage of a synchronous generator operating with a leading PF load (capacitive load). The increase in the terminal voltage can be justified by the fact that the armature reaction due to the leading PF load current is said to be magnetizing or strengthening the total air-gap flux. That is the reason that less amount of excitation (under-excitation) is required to return the terminal voltage to the desired rated value. Based on that, the voltage regulation has a negative value for a synchronous generator with leading PF load.

It can be concluded that the growth of unity and lagging power factor loads at synchronous generator terminals will require an increase in field excitation to maintain the generator's terminal voltage within the desired limits. In contrast, the field excitation may need to be reduced to keep the required terminal voltage for leading power factor loads.

It should be emphasized that the opposite of the above discussion is true for a motor action synchronous machine. Thus, for a synchronous motor, the armature reaction increases the main air-gap flux for the lagging power factor stator current (under-excitation mode) and decreases the flux for the leading power factor stator current (over-excitation mode) [57].

3.6 D-Q Axis Analysis of Salient-Pole Synchronous Generator

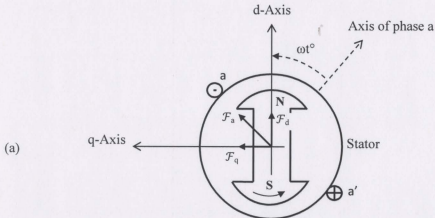
So far, initial consideration has been given to the cylindrical rotor theory where all the armature inductances and thereby the synchronous reactance were assumed to be a constant, regardless of the rotor position, due to the uniform air-gap geometry. In addition, both the armature and main-field flux waves were to act on the same magnetic circuit for the same reason. In a salient-pole generator, this, however, cannot be the case because of the saliency effect of the rotor. Thus, the non-uniform air-gap of the salient-pole generator will cause the air-gap inductances and reactances to be time-varying based on the rotor angular position with regard to the armature rotating mmf wave. Consequently, the armature reaction flux created in the air-gap by the stator current cannot be the same at any instant of time. This fact makes the analysis of such salient-pole electric machines even more complicated and needs careful consideration.

3.6.1 Flux and MMF Waveforms in a Salient-Pole Synchronous Generator

Two-reaction theory was proposed by Andrew Blondel as an effective approach to analyze the theory of salient-pole synchronous machines [6]. Its principle is to separate all the machine variables (fluxes, currents and voltages) into two mutually perpendicular

components acting along two different axes on a salient-pole rotor. The two relevant axes, as shown in Fig.3.6, are commonly called the direct axis and quadrature axis, and are denoted by d-axis and q-axis, respectively. The former (d-axis) is aligned with the axis of symmetry of a field pole while the other (q-axis) exists in the region midway between the salient poles (inter-polar air-gap space). It is arbitrarily chosen, based on the IEEE standard definition [60], that the q-axis leads the d-axis by 90° . With this in mind, the armature mmf (\mathcal{F}_a) due to the stator current can be resolved into two different components as indicated in Fig.3.6(a); one acts along the d-axis (\mathcal{F}_d) whereas the other (\mathcal{F}_q) acts along the q-axis of the salient pole rotor.

Since it coincides with the field pole axis and is thereby assumed to act over the same magnetic circuit as the field mmf, the (\mathcal{F}_d) component of the armature mmf distributes similarly to the main field mmf and may result in either a magnetizing or demagnetizing effect. The (\mathcal{F}_q) component, as its magnetic effect is found in the space between the salient poles, distributes quite differently from the field mmf and may therefore cause a cross-magnetizing effect [58].



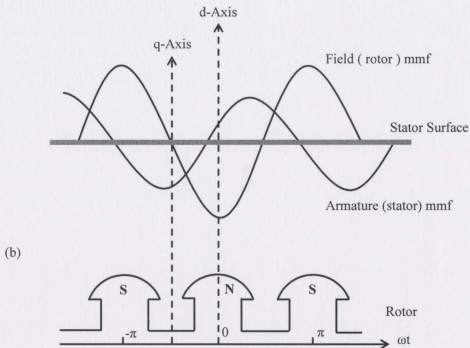


Fig.3.6 mmfs distribution in a salient-pole synchronous generator: (a) physical view (only phase-a is shown on the stator), (b) space-fundamental mmf waves with the respective d-q axes [60]

The space-fundamental armature mmf and field mmf waves distributing in a salient-pole generator are shown in Fig.3.6(b) with both the stator and rotor structure rolled out for clarity.

Accordingly, the armature reaction effect can be accounted for by two corresponding magnetizing reactances; d-axis armature reaction reactance (X_{ad}) and q-axis armature reaction reactance (X_{aq}). The leakage reactance of the armature winding (X_l) is the same for both the direct and quadrature axis (since it is independent of the rotor angle) and

therefore can be equally added to the armature reaction reactance to obtain the synchronous reactance components as:

$$X_d = X_{ad} + X_l \quad (3.11)$$

$$X_q = X_{aq} + X_l \quad (3.12)$$

where

X_d is the direct axis synchronous reactance.

X_q is the quadrature axis synchronous reactance.

Because of the saliency of the rotor, the established air-gap flux due to a given armature mmf (\mathcal{F}_a) will be created more at some points than others. In other words, the armature flux is greater in the short air-gap along the d-axis and smaller in the longer air-gap between the salient poles along the q-axis, ($\varphi_d > \varphi_q$). In fact, this aspect takes place because the air-gap magnetic reluctance of the flux path is smaller for the polar or d-axis than that for the inter-polar or q-axis, ($\mathcal{R}_d < \mathcal{R}_q$). This also explains the reason why the direct axis synchronous reactance (X_d) is larger than the quadrature axis synchronous reactance (X_q) [1].

3.6.2 Phasor Diagram Representation

The steady-state phasor diagram for a salient-pole synchronous generator based on two-axis theory is set forth and shown in Fig.3.7. The diagram considers the lagging power factor load case. It is of interest at this stage to derive the steady-state voltage equation using the developed phasor diagram.

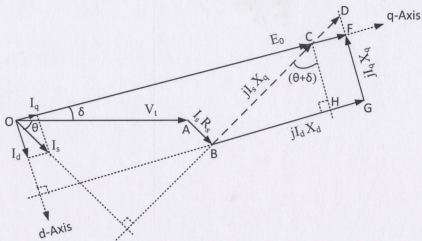


Fig.3.7 d-q axis steady-state phasor diagram of a salient pole synchronous generator with lagging power factor load

As seen in Fig.3.7, the stator current (I_s) has two orthogonal components centred on the d-axis and q-axis. These components are defined as:

$$I_d = I_s \sin (\delta + \theta) \quad (3.13)$$

$$I_q = I_s \cos (\delta + \theta) \quad (3.14)$$

Thus,
$$\vec{I}_s = I_d + j I_q \quad (3.15)$$

It must also be noticed that the q-axis component of the stator current I_q is in phase with the induced voltage vector (\vec{E}_g) whereas the d-axis component I_d is in time-quadrature (90°) with it. In the case of no-load, the only generated voltage in the stator winding is that induced by the field excitation (\vec{E}_g) [62]. However, if a load is connected, the armature reaction associated with d-axis and q-axis armature currents will cause two

relevant components of voltage to be induced in the stator windings. Each of these voltages lags by 90° behind the stator current component producing it and can be given as:

$$\bar{E}_d = -j X_{ad} \bar{I}_d \quad (3.16)$$

$$\bar{E}_q = -j X_{aq} \bar{I}_q \quad (3.17)$$

As a result, the net generated voltage per one phase in the stator winding is the phasor sum of the induced emf due to the field excitation plus both the components of the armature reaction voltage on d-axis and q-axis. Thus,

$$\bar{E}_t = \bar{E}_g + \bar{E}_d + \bar{E}_q = \bar{E}_g - j X_{ad} \bar{I}_d - j X_{aq} \bar{I}_q \quad (3.18)$$

Again, the total generated voltage is also equal to the phasor sum of the terminal voltage (\bar{V}_t) and the voltage drop in the armature winding. Hence,

$$\bar{E}_t = \bar{V}_t + \bar{I}_s (R_s + jX_l) \quad (3.19)$$

Comparing Eq.(3.18) with Eq.(3.19), the phasor excitation voltage or induced emf can be found as:

$$\bar{E}_g = \bar{V}_t + \bar{I}_s (R_s + jX_l) + j X_{ad} \bar{I}_d + j X_{aq} \bar{I}_q \quad (3.20)$$

Noting the Eqs.(3.11 and 3.12); this can be written in terms of the synchronous reactance components as the following:

$$\bar{E}_g = \bar{V}_t + \bar{I}_s R_s + j X_d \bar{I}_d + j X_q \bar{I}_q = E_g \angle \delta^\circ \quad (3.21)$$

For more clarity, a similar expression for the induced voltage equation can be derived referring to the Fig.3.7 as follows:

The magnitude of the induced voltage phasor (\vec{E}_g) in Fig.3.7 is equal to the length (\overline{OF}).

Thus,

$$E_g = \overline{OF} = \overline{OC} + \overline{CF} \quad (3.22)$$

Let the length (\overline{OC}) be equal to the magnitude of the vector (\vec{E}_0) and defined from the phasor diagram as:

$$\overline{OC} = |\vec{E}_0| = |\vec{V}_t + \vec{I}_s (R_s + jX_q)| \quad (3.23)$$

where \vec{I}_s is defined as in Eq.(3.15).

Moreover, from the phasor diagram the length (\overline{BC}) equals the quantity ($I_s X_q$), and similarly (\overline{BD}) equals ($I_s X_d$). Now, the length (\overline{CF}) can be found as:

$$\overline{CF} = |\overline{BG} - \overline{BH}| \quad (3.24)$$

or
$$\overline{CF} = |I_s X_d \sin(\delta + \theta) - I_s X_q \sin(\delta + \theta)| \quad (3.25)$$

$$\overline{CF} = |I_d (X_d - X_q)| \quad (3.26)$$

The final expression of the per-phase induced voltage can now be obtained by substituting the Eqs. (3.23 and 3.26) into Eq. (3.22) so:

$$E_g = |\vec{V}_t + \vec{I}_s (R_s + jX_q)| + |I_d (X_d - X_q)| \quad (3.27)$$

Note that the above equation calculates only the magnitude or rms value of the induced voltage. The direction of \vec{E}_g or the power angle (δ°) can be obtained from the phasor diagram as follows:

The stator current for the lagging pf load can be expressed as:

$$\vec{I}_s = I_s \angle -\theta^\circ = I_s \cos\theta - j I_s \sin\theta \quad (3.28)$$

Since \vec{E}_0 is in phase with \vec{E}_g , the power angle (δ°) may be found substituting the above value of the stator current into Eq.(3.23) as:

$$\vec{E}_0 = \vec{OC} = \vec{V}_t + (R_s + jX_q)(I_s \cos\theta - j I_s \sin\theta) \quad (3.29)$$

$$\vec{E}_0 = (V_t + I_s X_q \sin\theta + I_s R_s \cos\theta) + j(I_s X_q \cos\theta - I_s R_s \sin\theta) \quad (3.30)$$

$$\delta = \tan^{-1} \frac{I_s X_q \cos\theta - I_s R_s \sin\theta}{V_t + I_s X_q \sin\theta + I_s R_s \cos\theta} \quad (3.31)$$

Neglecting the stator resistance for large synchronous generators, the power angle can be rewritten as:

$$\delta \cong \tan^{-1} \frac{I_s X_q \cos\theta}{V_t + I_s X_q \sin\theta} \quad (3.32)$$

3.6.3 Steady-State Power-Angle Characteristic

The phasor diagram provided in the previous section can be used for the sake of deriving the expression of the power developed by a salient-pole synchronous generator. The curve that describes the real output power as a function of the power angle (δ°) is called the *power-angle characteristic* of a synchronous generator as shown in Fig.3.8.

The total three-phase output power delivered by a salient-pole synchronous generator consists of two components resulting from the d-q axis components of the stator current and voltage. Hence,

$$P_{3\phi} = P_d + P_q \quad (3.33)$$

or
$$P_{3\phi} = 3V_t I_d \sin\delta + 3V_t I_q \cos\delta \quad (3.34)$$

Alternatively, the same power equation can be obtained from the phasor diagram in Fig.3.7 as:

$$P_{3\phi} = 3V_t I_s \cos\theta \quad (3.35)$$

However,

$$I_s \cos\theta = I_d \cos(90^\circ - \delta) + I_q \cos\delta = I_d \sin\delta + I_q \cos\delta \quad (3.36)$$

$$\therefore P_{3\phi} = 3V_t I_d \sin\delta + 3V_t I_q \cos\delta \quad (3.37)$$

Also,

$$E_g = \overline{OF} = V_t \cos\delta + I_s R_s \cos(\theta + \delta) + I_d X_d \quad (3.38)$$

and
$$I_q X_q = V_t \sin\delta + I_s R_s \sin(\theta + \delta) \quad (3.39)$$

For large synchronous generators, $R_s \ll (X_d, X_q)$ and thus it is ignored, then we have:

$$I_d = \frac{E_g - V_t \cos\delta}{X_d} \quad (3.40)$$

$$I_q = \frac{V_t \sin\delta}{X_q} \quad (3.41)$$

Substituting Eqs.(3.40 and 3.41) into Eq.(3.37) and using the trigonometric identity:

$$\sin 2\delta = 2 \sin\delta \cos\delta \quad (3.42)$$

or

$$\sin\delta \cos\delta = \frac{1}{2} \sin 2\delta \quad (3.43)$$

Finally, the output power relation for a salient-pole synchronous generator is thus:

$$P_{3\phi} = \frac{3E_g V_t}{X_d} \sin\delta + \frac{3V_t^2}{2} \left(\frac{X_d - X_q}{X_d X_q} \right) \sin 2\delta \quad (3.44)$$

The above equation is the expression of the power-angle characteristic curve of a salient-pole synchronous generator. It gives the three-phase output power of the generator when the voltage and reactance quantities are used as the per-phase basis. The first part of the right-hand side of Eq.(3.44) represents the developed electric power due to the field excitation of the synchronous generator, whereas the second part, which is totally independent of the field excitation, is known as the *reluctance power* of the salient-pole synchronous generator. The resultant power is thereby the algebraic sum of the electric and reluctance power as shown in Fig.3.8. The reluctance power is basically an additional power generated due to the variations in the air-gap magnetic reluctances as a function of the rotor position (i.e. the power developed due to the saliency effect). This power will in turn develop a torque of its own known as the *reluctance torque*. Only at small excitation does the reluctance power or torque have a significant impact. If that is not the case, the analysis of a salient-pole synchronous machine may otherwise be made on the same basis as the cylindrical rotor theory [58].

The machine is still able to develop power or torque even when the excitation is removed. However, it is obvious that if the saliency is neglected (i.e. $X_d = X_q$), the reluctance power would disappear and one would end up with the first term of Eq.(3.44) alone, which is in fact the same as the power developed by a cylindrical rotor (nonsalient-pole) synchronous generator.

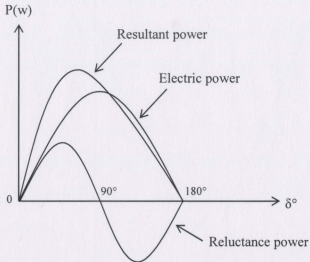


Fig.3.8 Steady-state power-angle characteristic of a salient-pole synchronous generator

3.7. Synchronous Generator Transients

The previous discussions are explicitly concentrated on the steady-state operation of a synchronous generator. The machine behaviour is however quite different during disturbances or abnormal conditions. Disturbances may occur for many reasons such as the accidental occurrence of symmetrical or unsymmetrical faults, or a sudden change in the mechanical torque on the generator shaft or in the electric load applied to the generator terminals and so forth. A synchronous generator is most likely to lose its

synchronism during these awkward conditions unless certain procedures are quickly done.

The synchronous generator response or behaviour during the disturbances is known as *synchronous generator transients*. The synchronous generator transients can be either electric transient or mechanical (dynamic) transient in nature. The time needed by the generator to overcome the transient operation and return to its steady-state operation is called the transient period which may last for a finite period of time. The principle reason for the increased chance of losing the generator synchronism during the transient period is that the speed oscillation, also called *hunting*, would take place on the rotor shaft due to the fluctuation of the rotor around its new angular position (torque-angle) making the rotor speed up and thus pulling it out of the synchronism. Various techniques are applied by synchronous machines designers to reduce the hunting phenomenon effect; among them are the use of damper windings and fly wheels [57].

3.7.1 Steady-State Direct-Axis and Quadrature-Axis Synchronous Reactances (X_d and X_q)

It has already been noted that the direct and quadrature axis synchronous reactance mentioned in the preceding sections were intended only for the steady-state operation where a positive sequence armature current was to flow in the stator windings after reaching its sustained value. At this point, it is desirable to visualize the physical definition of these steady-state synchronous reactances. To do so, consider that a positive-sequence (steady-state) stator current is applied at an instant of time when the rotor is

synchronously driven and in a position so that its polar or direct axis is directly in line with the peak of the rotating armature fundamental mmf. Also, assume that this current is acting alone (all the field circuits are opened). As a result of this operation mode, a path of high permeance will be offered in the air-gap and thereby the flux linkage of the armature winding is the greatest for any rotor position. Under this condition, the ratio of the net armature flux linkage per one phase winding to the current through the same phase, times the angular frequency ($2\pi f$) yields the steady-state value of the direct-axis synchronous reactance (X_d) [63].

Similarly, the same stator current is now applied but at a different instant, at which the rotor has its interpolar or quadrature-axis aligned with the axis of the armature mmf wave. With this in mind, minimum air-gap permeance is therefore presented resulting in much smaller flux linkage of the stator windings. Under this condition, the offered air-gap reactance is the quadrature-axis steady-state synchronous reactance (X_q). It is apparent that ($X_d > X_q$).

3.7.2 Direct-Axis Transient and Subtransient Synchronous Reactances (X'_d and X''_d)

During the transient conditions, the components of the synchronous reactance would not have the same values as those for the steady-state conditions. Associated with transient value, suppose that a positive-sequence current is now suddenly applied to the stator windings. Furthermore, the rotor field winding is short-circuited and not excited (also, the damper circuit, if found, is somehow opened). The rotor is synchronously driven and in a position such that its direct-axis is in line with the stator mmf wave. The current will be

induced in the closed field circuit opposing the suddenly appearing armature mmf and tending to keep the field linkage at almost zero (constant flux linkage law: *the total flux linkage in any closed electrical circuit cannot be changed instantly*) at the first short duration [63]. Therefore, the armature flux will be alternatively restricted to the low permeance path offered by the interpolar space. The net armature flux linkage is thereby less than that in the steady-state condition. If that is the case, the ratio of the total armature flux linkage to the armature current per phase times the angular frequency ($2\pi f$) gives the direct-axis transient synchronous reactance (X'_d). It should be emphasized that the transient current induced in the field windings will decay to zero after just a short time from the appearance of the suddenly applied armature current due to the field winding resistance.

For the subtransient direct-axis reactance, the exact same conditions specified for defining (X'_d) are still valid except that the damper circuit effect would definitely take place. Thus, during the subtransient interval, besides the current induced in the closed field windings, an extra current will also be induced in the shorted damper windings. Because those windings are in a position that is, compared to the field windings, closer to the armature structure, the armature flux linkage per phase winding is much less than that which corresponds to the transient period. The associated armature winding reactance due to such a case is referred to as the direct-axis subtransient synchronous reactance (X''_d). Again, the subtransient current induced in the damper windings will die out more rapidly than that induced in field windings due to the comparatively higher resistance of the damper windings. It is evident that for a salient-pole synchronous generator with damper

or amortisseur windings ($X_d > X'_d > X''_d$), whereas ($X'_d \cong X''_d$) for one without damper windings [64].

3.7.3 Quadrature-Axis Transient and Subtransient Synchronous Reactances (X'_q and X''_q)

The conditions for defining the transient and subtransient quadrature-axis synchronous reactance are quite analogous to those specified above for both transient and subtransient direct-axis synchronous reactance. The only difference between the two cases lies in the rotor position at the time the sudden positive-sequence armature current is applied. Hence, for X'_q and X''_q , it is assumed that the armature current is suddenly applied at such an instant that the rotor is synchronously rotated so that its quadrature-axis (interpolar space) is now aligned with the axis of the rotating armature mmf wave. Likewise, a similar definition for both quadrature-axis reactances can be given.

For the transient value, consider the same assumptions that the field windings are unexcited and closed and the damper or amortisseur windings, if found, are imagined to be open. In this case, unlike the direct-axis transient reactance case, the current will not be induced in the closed field windings as the field linkage due to the armature flux is already zero. Therefore, the armature flux will distribute through the same low permeance path between the field poles as that presented in the definition of the quadrature-axis steady-state synchronous reactance. The presented synchronous reactance due to such conditions is the quadrature-axis transient synchronous reactance (X'_q). It can therefore be written that ($X_q \approx X'_q$) for a laminated salient-pole synchronous generator. For a solid

rotor synchronous machine, this comment is incorrect, because the transient currents might be induced in the rotor core, making $(X'_q < X_q)$.

For the subtransient value, the damper windings are assumed to be close-circuited in addition to the closed field windings. In this respect, a subtransient current will flow in the damper circuit trying to maintain its flux linkage at approximately zero and thereby making the armature flux pass through the minimum permeance path of the interpolar space. The result of this is much lower net armature flux linkage in one phase winding per ampere. The corresponding quadrature-axis reactance is then the quadrature-axis subtransient synchronous reactance (X''_q) . In general, for a salient-pole synchronous generator with no damper windings $(X_q = X'_q = X''_q)$ [63].

3.8 Potier Reactance Concept

Potier reactance, denoted by (X_p) , is a fictitious reactance that comprises the armature leakage flux and the extra leakage flux of the field windings due to the field current of a synchronous machine [28]. It is sometimes used instead of the armature leakage reactance (X_l) in the phasor representation of synchronous machines. For a solid (cylindrical) rotor synchronous machine, the Potier reactance is almost equal to the stator leakage reactance. However, it is often greater than the stator leakage reactance for one of a salient-pole type. The purpose of employing this reactance is to determine the armature reaction voltage drop for any given load current. The Potier reactance cannot be directly measured. Nevertheless, it can be obtained graphically from both the no-load saturation

curve and the zero-power factor rated current saturation curve; (*Potier Triangle Method*) as will be provided later on.

In the determination of the steady-state and transient parameters of a synchronous machine, a variety of tests may be conducted. The IEEE and IEC organizations have published a standardized guide to describe those tests in great detail; [27] and [28], respectively. The most commonly used test among the group is the sudden three-phase short circuit. This test can provide accurate enough results that help to investigate the machine behaviour during the transient conditions. The sudden three-phase short circuit test is carried out in the laboratory on a practical salient-pole synchronous generator as a part of the contribution of this thesis.

Chapter 4

Experimental Determination of Synchronous Machine Parameters

In the foregoing part of this thesis, a reasonable effort has gone into providing a clear picture about the synchronous machine theory, especially the theory of a salient-pole synchronous machine. Now, it is time to introduce the essential work which has been done in this research. This chapter presents the experimental test results that were obtained in the laboratory by performing particular tests to determine the machine parameters of a salient-pole synchronous generator. The main aim is to find the steady-state and transient direct-axis synchronous reactance as well as the armature reaction voltage drop (*Potier reactance voltage drop*) for the synchronous generator to be tested.

4.1 The Electric Machine under Consideration



Fig.4.1 Laboratory salient-pole synchronous machine

The machine being treated, as shown in Fig.4.1, is a salient-pole synchronous generator with damper bar windings. The nameplate quantities of this synchronous generator are:

3-phase 2 KVA, 208 V (line-to-line), 4-pole, 1800 rpm, 60 Hz, 5.5 A, PF: 0.8

In Fig.4.1, the machine to the left-hand side is a dc motor (shunt connection) that is used as a prime mover for the synchronous generator on the right-hand side. Also, it can be seen that a rheostat is connected to the armature circuit of the dc motor to achieve more adjustable speed control.

4.2 The Base Impedance

It is always convenient to calculate machine parameters on a per-unit basis as this has been the usual practice in electric machinery design and analysis. Therefore, before proceeding in this chapter, it is better to first determine the base impedance (Z_b) for the studied generator. This can be done using the given rated values as follows:

$$Z_b = \frac{V_{b \text{ rated (L-L)}}}{\sqrt{3} \times I_{b \text{ rated}}} \quad (4.1)$$

$$Z_b = \frac{208}{\sqrt{3} \times 5.5} = 21.83 \Omega$$

Then, the per-unit reactance is defined as:

$$X_{pu} = \frac{X_{\text{actual}} (\Omega)}{Z_b} \quad (4.2)$$

4.3 Measurement of Stator Resistance R_s

As outlined earlier in chapter three (Sec.3.4) the per-phase ac stator resistance for Y-connected stator windings can be found as follows:

$$R_s = \frac{1}{2} R_{dc(L-L)} \times 1.6 \quad \Omega \quad (4.3)$$

where R_{dc} is the average line-to-line dc resistance that was measured to be (2.2 Ω) for the tested generator. It is to be noted that 1.6 is the skin effect of the alternating stator current for 60 Hz operation. Therefore,

$$R_s = \frac{1}{2} \times (2.2) \times (1.6) = 1.76 \Omega = 0.081 \text{ pu}$$

4.4 The Performed Standard Tests

The tests conducted on the chosen electric machine in this thesis are:

- 1- Open-Circuit Test.
- 2- Sustained Short-Circuit Test.
- 3- Slip Test.
- 4- Zero Power-Factor Test.
- 5- Sudden Three-Phase Short-Circuit Test.

All five tests are discussed in full detail with an analytical approach in the next sections. The test results from the first two tests are provided together since they are complementary to each other and need to be simultaneously presented. The rest of the results are however introduced individually.

4.4.1 Open-Circuit Test

The open-circuit test is carried out on a synchronous generator at no load. The reason is to obtain the no-load saturation curve, or as commonly termed, the *Open-Circuit Characteristic (OCC)* for the tested synchronous generator. Thereafter, the *OCC* is used

graphically to determine the saturated and unsaturated steady-state values of the synchronous reactance as well as the machine *Short-Circuit Ratio (SCR)*. The short-circuit ratio (*SCR*) for a synchronous generator is defined as the ratio of the field current required to obtain the rated terminal voltage at open circuit to the field current required for the rated armature current at short circuit .

Test Procedures

During the open-circuit test, the rotor of the unloaded generator is first run at its rated synchronous speed of 1800 rpm with no excitation being applied to the rotor (field) windings. The field current is then gradually supplied to the field windings while measuring the open-circuit terminal voltage till reaching its saturation condition (i.e. the generated voltage increases very slowly or not at all with the increase in the field current). The readings of the no-load terminal voltage versus the field current are recorded. After finishing, a curve of the no-load terminal voltage with the change in the field current is plotted using the test data as shown in Fig.4.2. This curve represents the no-load saturation curve or the open-circuit characteristic (*OCC*) for the tested generator. The no-load saturation curve obeys a linear relationship (straight line) as long as the machine's magnetic core is not yet saturated. The extension of this straight portion for higher values of the field current gives the air-gap line.

4.4.2 The Sustained Short-Circuit Test

The object of the sustained short-circuit test is to find the short-circuit saturation curve or the so-called *Short-Circuit Characteristic (SCC)* for a synchronous generator. This curve is then used with the no-load saturation curve for the same purpose. One has to keep an

eye on the value of the stator current not to exceed its rated value while performing this test. Generally, during the test, the rated value of the stator current of the tested generator might be exceeded by only a small tolerance to avoid stator windings damage.

Test Procedures

The generator under test is operated at the rated synchronous speed with its stator terminals permanently short-circuited through a proper switching assembly. The field current is then gradually increased while measuring the short-circuit current flowing in the stator windings. The variation of the short-circuit stator current with the field current yields the short-circuit characteristic (*SCC*) of the tested generator. The field current reading at which the rated stator current is obtained should be precisely recorded for finding the value of the short circuit ratio (*SCR*) as will be provided later on. The *SCC* for the tested generator is shown below in Fig.4.2.

➤ Experimental Results from the Open-Circuit and Short-Circuit Tests

The following table provides the test data obtained from the open- and short-circuit tests:

Table.4.1 Test data from open- and short-circuit tests

<i>Field Current (A)</i>	0.1	0.2	0.3	0.4	0.5	0.7	0.81	0.9	1.5	1.6
<i>L-L Terminal Voltage (V)</i>	30	56	82	111	137	187	208	223	274	279
<i>OC Test</i>										
<i>Field Current (A)</i>	0.1	0.2	0.3	0.4	0.53	0.6	0.7			
<i>Armature Current (A)</i>										
<i>SC Test</i>	1.2	2.2	3.25	4.26	5.5	6.25	7.28			

From the above table the following graph is plotted:

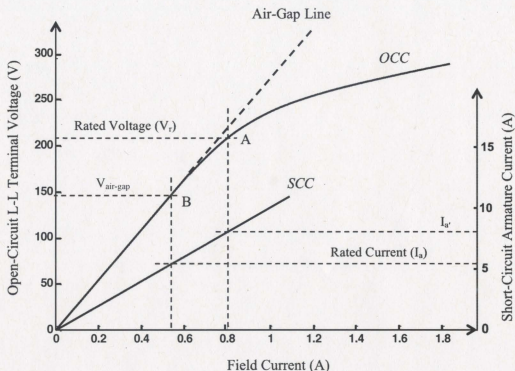


Fig.4.2 Open- and Short-Circuit Characteristics for the laboratory synchronous generator

The direct-axis saturated synchronous impedance $Z_{d(sat)}$ can be determined from point A with reference to Fig.4.2. This point corresponds to the no-load rated voltage on the open-circuit characteristic. Therefore, $Z_{d(sat)}$ is obtained as a quotient of the rated voltage on the OCC (taken at point A) and the short-circuit armature current on the SCC corresponding to the field current at the same point, as can be seen in Fig.4.2. Thus,

$$Z_{d(sat)} = \frac{V_{T \text{ rated (L-L)}}}{\sqrt{3} \times I_{SC \text{ corresponding to the field current at rated voltage}}} \quad (4.4)$$

thus,
$$Z_{d(sat)} = \frac{V_r}{I_{a'}} = \frac{208}{\sqrt{3} \times 8.32} = 14.43 \Omega$$

The direct-axis saturated synchronous reactance $X_{d(sat)}$ is therefore:

$$X_{d(sat)} = \sqrt{Z_{d(sat)}^2 - R_s^2} \quad (4.5)$$

$$X_{d(sat)} = \sqrt{(14.43)^2 - (1.76)^2} = 14.32 \Omega$$

In per-unit,

$$X_{d(sat)} = \frac{X_{d(sat) \text{ actual}}}{Z_b} \quad (4.6)$$

$$X_{d(sat)} = \frac{14.32}{21.83} = 0.656 \text{ pu}$$

The direct-axis unsaturated synchronous impedance $Z_{d(unsat)}$ can be found in a similar way, though from any point on the air-gap line, such as point B in Fig.4.2 which corresponds to the field current for rated short-circuit armature current. Then,

$$Z_{d(unsat)} = \frac{V_{\text{air-gap (L-L)}}}{\sqrt{3} \times I_{a \text{ SC rated}}} \quad (4.7)$$

$$Z_{d(unsat)} = \frac{147}{\sqrt{3} \times 5.5} = 15.43 \Omega$$

The direct-axis unsaturated synchronous reactance $X_{d(unsat)}$ is:

$$X_{d(unsat)} = \sqrt{Z_{d(unsat)}^2 - R_s^2} \quad (4.8)$$

$$X_{d(unsat)} = \sqrt{(15.43)^2 - (1.76)^2} = 15.33 \Omega = 0.702 \text{ pu}$$

It should be mentioned that both of the reactance values, just calculated above, are only intended for the steady-state condition.

The short-circuit ratio SCR is given as:

$$SCR = \frac{I_f(\text{at OC rated voltage})}{I_f(\text{at SC rated current})} \quad (4.9)$$

$$SCR = \frac{0.81}{0.53} = 1.528$$

One should note that the reciprocal of the SCR is equal to the saturated value of the d-axis synchronous reactance expressed in per unit!

4.4.3 The Slip Test

The objective of the slip test is to find the value of the quadrature-axis synchronous reactance X_q by finding the *saliency ratio* (X_q/X_d). This ratio is then to be multiplied by the value of the direct-axis synchronous reactance X_d obtained from the open-circuit and short-circuit characteristics to compute the quadrature-axis synchronous reactance X_q . If a saturated value of X_d is used, the result will be a saturated value of X_q . A similar statement can be made if an unsaturated value of X_d from the open-circuit and short-circuit characteristics is used.

Test Procedures

During the slip test, the generator being tested is driven by means of a prime mover at a speed slightly different from the synchronous speed, about 1% more or less, to achieve a

very small slip. The field windings on the rotor must be kept open-circuited so that current is not induced in them. Thereafter, a balanced three-phase voltage is applied across the generator terminals. At this point, the applied voltage should not be more than approximately 25% of the rated voltage of the generator [57]. An oscillogram of the reduced armature (stator) voltage and current can then be recorded as shown in Fig.4.3.

➤ Experimental Results from the Slip Test

Fig.4.3 shows the oscillation of the stator current and voltage for the tested generator during the slip test. It can be clearly noticed from this figure that both the stator voltage and current oscillate, having minimum and maximum values as time passes.

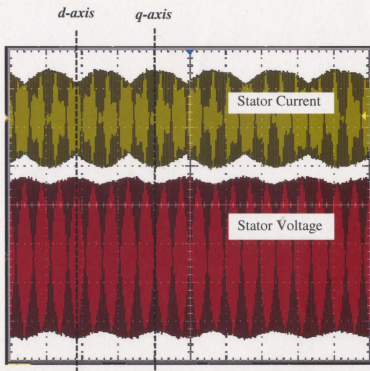


Fig.4.3 Typical oscillogram from the slip test

At an instant of time when the stator voltage has its maximum amplitude, the stator current has its minimum value. This is the time when the rotor has its direct-axis in line with the armature magnetomotive force mmf and thereby the offered air-gap reactance represents the direct-axis synchronous reactance. In a similar manner, at the moment when the stator voltage is minimum, the stator current is maximum. The rotor quadrature-axis at this specific time is aligned with the armature mmf and thus the presented air-gap reactance is the quadrature-axis synchronous reactance [64].

From the stator current and voltage waveforms found from the slip test, the following calculations can be made.

$$X_{d(stip)} = \frac{V_t(L-L) \max}{\sqrt{3} \times I_{\min}} \quad (4.10)$$

$$X_{d(stip)} = \frac{63}{\sqrt{3} \times 9.5} = 3.83 \Omega$$

$$X_{q(stip)} = \frac{V_t(L-L) \min}{\sqrt{3} \times I_{\max}} \quad (4.11)$$

$$X_{q(stip)} = \frac{52.2}{\sqrt{3} \times 12.5} = 2.41 \Omega$$

The saliency ratio is thus

$$\left[\frac{X_q}{X_d} \right]_{stip} = \frac{2.41}{3.83} = 0.63 \quad (4.12)$$

Finally, as mentioned earlier, the saliency ratio can be used with the X_d value previously obtained from OCC and SCC to compute the actual steady-state saturated and unsaturated value of the quadrature-axis synchronous reactance for the tested generator. That is,

$$X_q = X_d \times \left[\frac{X_q}{X_d} \right]_{slip} \quad (4.13)$$

$$X_{q(sat)} = 14.32 \times 0.63 = 9.02 \, \Omega = 0.413 \, pu$$

and

$$X_{q(unsat)} = 15.33 \times 0.63 = 9.66 \, \Omega = 0.442 \, pu$$

4.4.4 Zero Power-Factor Test

This test is performed to obtain the zero power-factor saturation curve or, as it is called, the *Zero Power-Factor Characteristic (ZPFC)* that is used with the OCC to determine the armature leakage or Potier reactance drop (armature-reaction drop) for a synchronous generator at any given load current. The ZPFC is a graph of the terminal voltage against the field current with the stator current held constant (mostly at the rated value) and with zero lagging power factor operation ($\theta=90^\circ$). Consequently, the Potier reactance (defined in Ch.3, Sec.3.8) is found using any point on the ZPFC. It is often sufficiently accurate to use the point that corresponds to the rated voltage and rated current, as is the case in this research work [65].



Fig.4.4 Adjustable 3-phase reactor used as a load in the zero power-factor test

Test Procedures

The zero power-factor test is a straightforward test carried out by loading the tested generator with either a pure reactor (inductive load) or an underexcited synchronous motor to achieve a zero lagging power-factor loading condition. The two-wattmeter method is used to ensure zero delivered real power from the generator to the load during the test. The reactor used as a load for the tested generator is shown above in Fig.4.4. By a proper adjustment to the field excitation and the load, both at the same time, readings of the terminal voltage variation with the field current when a constant rated armature current is drawn can be measured in steps. From those readings, the zero power-factor characteristic ZPFC is developed as in Fig.4.5. If plotted together on one graph, it can be noticed that the ZPFC is nearly parallel to the OCC and shifted by a constant distance to the right.

➤ Experimental Results from the Zero Power-Factor Test

Provided below is the test data from the zero power-factor test conducted at rated stator current.

Table.4.2 Experimental test result from the zero power-factor test

<i>Field Current (A)</i>	0.53	1.32	1.38	1.4	1.55	1.81	2
<i>L-L Terminal Voltage (V)</i> <i>ZPFC Test</i>	0	205	208	210	228	250	258

The zero power-factor rated current saturation curve or (ZPFC) is plotted on the same graph with the previously obtained open-circuit characteristic (OCC) as shown in Fig.4.5 below.

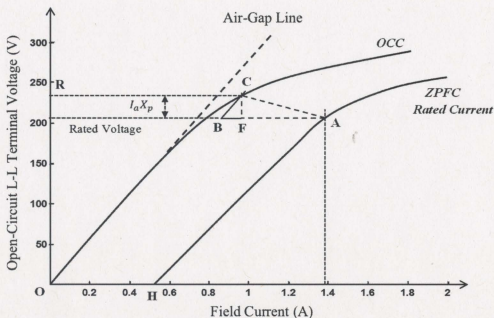


Fig.4.5 Potier triangle method for the laboratory salient-pole synchronous generator

❖ Determination of Potier Reactance (Potier Triangle Method)

The Potier reactance can be calculated in reference to Fig.4.5 by the following steps:

- First, the OCC and ZPFC are plotted against the dc excitation current on the same graph.
- Point A, the ordinate of which is the rated voltage, is determined on the ZPFC.
- To the left of A, a horizontal line BA equals OH is drawn towards the OCC. The length OH is equal to the field current corresponding to zero terminal voltage on the ZPFC. This field current is also equal to that needed to circulate the rated stator current under a sustained short-circuit condition [27].
- Line BC parallel to the air-gap line is drawn upwards from point B. The intersection of this line with the knee of the OCC is point C.
- From C, a perpendicular line is drawn downwards till it intersects with the line BA, at the point F. The formed triangle AFC between the two curves is known as the *Potier triangle*.
- Finally, the vertical leg CF of the Potier triangle represents the leakage or Potier reactance drop ($I_a X_p$) at the rated armature current. Thus, for the laboratory salient-pole synchronous generator:

$$\overline{CF} = I_a X_p = 22 \text{ V (line to line)} = 12.7 \text{ V (per phase)} \quad (4.14)$$

and therefore, the Potier reactance X_p (stator leakage reactance X_l) is equal to:

$$X_p = X_l = \frac{12.7}{5.5} = 2.31 \Omega = 0.106 \text{ pu}$$

- Adding the Potier reactance drop ($I_a X_p$) to the rated terminal voltage gives the length OR which represents the voltage behind Potier reactance E_p . Thus,

$$E_p = V_{t(\text{rated})} + I_a X_p \quad (4.15)$$

$$E_p = 208 + 22 = 230 \text{ V (line to line)}$$

With reference to Fig.4.5, the distance BA represents the total field current required to circulate the rated stator current at short-circuit condition. This current can be resolved into: the field current BF necessary to overcome the leakage reactance drop, and the current FA required to overcome the demagnetizing effects (armature reactions) of stator current.

The voltage drop due to the Potier reactance is $I_a X_p$. If the Potier triangle is slid down (i.e. Potier triangle is developed at a voltage value which is less than the rated terminal voltage), the Potier reactance voltage drop $I_a X_p$ would obviously be larger than that obtained at the rated terminal voltage which in turn results in less accurate approximation of the stator leakage reactance X_l . In fact, the quantity ($I_a X_p$) is comprised of both the armature reaction voltage drop and voltage drop due to stator leakage reactance. If the ZPFC is developed at value of stator current which is different from the rated value, the voltage drop due to armature reaction would vary, whereas that due to stator leakage reactance would remain constant.

4.4.5 Sudden Three-Phase Short-Circuit Test

One important aspect to visualize the behaviour of the synchronous generators during the dynamic and electric transients is the sudden three-phase short-circuit. Many of the transient and subtransient reactance parameters can be computed from a suitable oscillogram of a short-circuit current suddenly applied to the generator terminals. The interest here is to calculate the direct-axis transient and subtransient synchronous reactance X'_d and X''_d , respectively. The quadrature-axis transient and subtransient synchronous reactances are often of little significance during the short-circuit conditions [66], and therefore they are beyond the scope of this thesis.

Test Procedures



Fig.4.6 Test set up for the sudden three-phase short-circuit test.

The sudden three-phase short-circuit test is performed on the laboratory generator at rated terminal voltage and with no-load operation. That is, the tested salient-pole generator is driven at the synchronous speed and is excited so that the rated terminal voltage (208V) is obtained at a no-load condition. Thereafter, a three-phase short-circuit is suddenly applied at the generator terminals. The test set up is as shown in Fig.4.6.

❖ **Description of Three-Phase Short-Circuit Current**

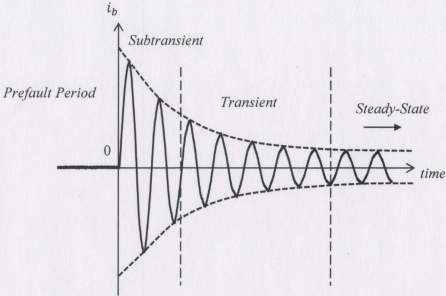


Fig.4.7 Typical short-circuit phase current waveform

Fig.4.7 shows a typical short-circuit current waveform suddenly flowing in one stator phase. It consists of two main components: one is a symmetrical or alternating component, the so-called ac component, while the second is the asymmetrical or unidirectional component (dc component). The ac component may in turn be resolved into three distinct periods of time, associated with them are three different components of

the short-circuit current. Those are the subtransient component I'' , transient component I' , and sustained or steady-state component I_s . The subtransient period results in the largest initial value of the short-circuit current, mainly caused by currents induced in damper windings, and lasting for a very short time (only the first few cycles) from the instant of the short-circuit. The transient period immediately follows the subtransient period and spans a relatively longer time. Right after and ultimately, the steady-state period does appear during which the short-circuit current approaches its sustained value [60].

It should be noticed from Fig.4.7 that the current waveform envelope obeys an exponential decay. Moreover, the decay is very fast at the first couple of cycles (the subtransient period) and gradually slows down during the following few cycles (transient period) till it becomes almost constant at the steady-state period. The time constant controlling the rapid decay during the subtransient period is called the direct-axis subtransient short-circuit time constant T''_d while that controlling the slower decay during the transient period is called the direct-axis transient short-circuit time constant T'_d . It is evident that T''_d is comparatively less than T'_d .

The unidirectional dc component of the short-circuit stator current is also exponentially decaying, though to zero, with a time constant known as the short-circuit armature time constant T_a . The initial value of each component depends on which point of the cycle the short-circuit takes place. Sometimes, the dc component results in an asymmetrical short-circuit current (thus, the current waveform has either a negative or positive dc-offset) unlike the current waveform shown in Fig.4.7.

In some cases, second harmonic components do exist (the value of which depends on the difference between X'_d and X''_d) in the short-circuit current, especially for a salient-pole generator without damper windings. For a generator with damper windings, subtransient currents would flow in them preventing the existence of the second harmonic armature currents. However, those components are normally very small and can be regarded as negligible [64].

From the above discussion, the rms amplitude of the total ac component of the short-circuit current in one phase at any instant of time can be defined as follows:

$$I_{sc}(t) = (I'' - I')e^{-t/T'_d} + (I' - I_s)e^{-t/T_d} + I_s \quad (4.16)$$

or

$$I_{sc}(t) = E_o \left[\left(\frac{1}{X'_d} - \frac{1}{X_d} \right) e^{-t/T'_d} + \left(\frac{1}{X_d} - \frac{1}{X_d} \right) e^{-t/T_d} + \frac{1}{X_d} \right] \quad (4.17)$$

where E_o is the rms line-to-neutral open-circuit prefault terminal voltage.

The initial value of the subtransient short-circuit current (I'') can be estimated by extending the line connecting the rapidly decaying peaks of the ac component back to the zero-time point or the instant of the short circuit. In a similar approach, the initial value of the transient short-circuit current (I') is found, although it neglects the rapidly decaying peaks as shown in Fig.4.10. The direct-axis transient and subtransient synchronous reactance X'_d and X''_d can now be found, with reference to Eqs. (4.16 and 4.17), as the

ratio of the prefault open-circuit voltage to the associated components of short-circuit current. That is,

$$X'_d = \frac{E_o}{I'} \quad (4.18)$$

$$X''_d = \frac{E_o}{I''} \quad (4.19)$$

The time constants T'_d and T''_d are defined as the time required for the related current component to decrease to $(1/e)$ or 0.368 times its initial value [65], as is clear from Fig.4.10.

The field current following the sudden short-circuit also has both ac and dc components. The ac component of the field current is said to be produced by the dc component of the stator current and thereby decays with the same time constant T_a . Conversely, the dc component of the field current can be regarded as the reason for the appearance of the ac component in the armature current [65]. The dc component of the field current, like the ac component of the armature current, also is comprised of transient, subtransient and steady-state components with the same associated time constants, T'_d and T''_d .

➤ Experimental Results from the Sudden Three-Phase Short-Circuit Test

The following test results were experimentally obtained from a sudden three-phase short-circuit developed at the terminals of the laboratory salient-pole synchronous generator at rated voltage for no load. Fig.4.8 shows the stator phase currents with the dc field current after the short circuit while Fig.4.9 indicates phase-b short-circuit stator current alone with the dc field current.

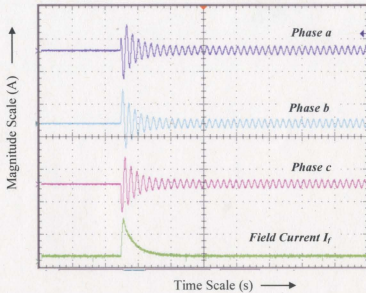


Fig.4.8 Currents oscillogram from sudden three-phase short-circuit test at 1 pu rated voltage

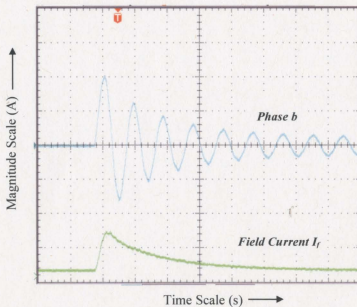


Fig.4.9 Phase-b short-circuit stator current alone with the dc field current at 1 pu rated voltage

Referring to the obtained test results as in Figs.4.8 and 4.9 the following discussion can be provided. Before the instant of short-circuit, the flux linkage of the excited field windings is constant whereas that of the armature windings is sinusoidally time-varying. Immediately after the short-circuit happens and by the principle of constant flux linkage, which states: "*the flux linkage of any closed circuit of finite resistance and e.m.f cannot change instantly*" [8], the suddenly appearing armature mmf will be resisted by a jump or sudden increase in the field current over its initial value before the short circuit as seen in Fig.4.8. In other words, the field current will be increased simultaneously at the short-circuit moment to overcome the demagnetizing effect of the large current and maintain the air-gap flux linkage constant for a short time following the short-circuit [65]. Subtransient current flows in the damper windings for similar reasons. This current would however die out very rapidly due to the high resistance of damper windings. Again, as per the theorem of constant flux linkage, the terminal voltage is zero at the short circuit. The change of flux linkage with the stator current must also be zero [63]. This fact justifies the large initial values of the short-circuit current; that is, current components must be induced in the stator windings in order for the air-gap flux linkage to remain constant for a short time after the short-circuit.

The phase-b current waveform in Fig.4.9 is used to obtain the exponential decay or the envelope of the short-circuit current. A set of points which are the positive peaks of this phase current is estimated whereby the short-circuit current envelope is drawn as shown in Fig.4.10. Polynomial curve-fitting technique using Matlab was applied to obtain an accurate shape of the current envelope around the selected points indicated by the nodes

or script “o” in Fig.4.10. As pointed out earlier, by extrapolating the subtransient and transient current envelope back to zero-time or the time of the short-circuit occurrence, the subtransient and transient current components can be evaluated, whereby X'_d and X''_d are determined.

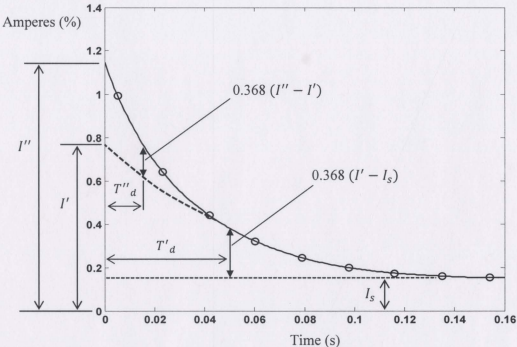


Fig.4.10 Polynomial curve fitting of phase-b short-circuit current envelope

Therefore, X'_d and X''_d are determined using Eqs. (4.18 and 4.19) as follows:

$$X'_d = \frac{208}{\sqrt{3} \times 53.03} = 2.26 \Omega = 0.104 pu$$

$$X''_d = \frac{208}{\sqrt{3} \times 80.61} = 1.49 \Omega = 0.068 pu$$

The time constants T'_d and T''_d are estimated to be 50ms and 15ms, respectively.

The total rms ac component of the short-circuit current can now be expressed, referring to Eq.(4.16), as a function of time as follows:

$$I_{sc}(t) = (27.58)e^{-t/0.015s} + (42.28)e^{-t/0.05s} + 10.75 \quad \text{Amps.}$$

4.5 Summary

The following table summarizes the parameters that have been determined for the laboratory synchronous generator.

Table.4.3 Measured constants for the laboratory salient-pole synchronous generator

<i>Parameter</i>	<i>Quantity (per unit)</i>
R_s	0.081
$X_{d(sat)}$	0.656
$X_{d(unsat)}$	0.702
$X_{q(sat)}$	0.413
$X_{q(unsat)}$	0.442
X'_d	0.104
X''_d	0.068
X_p	0.106
T'_d	0.05 (s)
T''_d	0.015 (s)

Chapter 5

Conclusion and Future Work

5.1 Conclusion

This research work has been devoted to the experimental determination of equivalent circuit parameters for a laboratory salient-pole generator. Direct-axis synchronous reactance as well as stator leakage reactance are of paramount importance for synchronous machine analysis and design as the synchronous machines performance during steady-state and transient operation is, in particular, largely affected by these parameters. The investigation starts by providing a clear insight into the scope of synchronous machines theory. At this point, special attention has been given to the synchronous generator of a salient-pole type as it is the machine being dealt with in this thesis. Thereafter, a set of standard tests as defined by the IEEE standard 115-1995 is conducted in the laboratory for the purpose of the estimation of the machine parameters. The experimental test results are then analyzed, whereby the required machine parameters are extracted. The accurate determination of synchronous machine parameters has increasingly been a fascinating challenge to face for graduate scholars as well as professional machine designers.

5.2 Future Work

The further work that would be suggested in regard to this thesis is that verification of the obtained machine parameters using the available engineering software would be of

References

- [1] Turan Gonen, "Electrical Machines with Matlab", Second edition, CRC Press, Taylor & Francis Group, LLC, 2012.
- [2] O.E. Mainer, "The Nature of Synchronous Reluctance of a Cylindrical-rotor Alternator", *Journal IEE*, Vol.7, No.76, pp.224-225, April 1961.
- [3] R. H. Park, "Two-Reaction Theory of Synchronous Machines- Generalized Method of Analysis- Part I", *AIEE Trans.*, Vol.48, No.3, pp.716-727, July 1929.
- [4] S. K. Baik, M. H. Sohn, E. Y. Lee, Y. K. Kwon, T. S. Moon, H. J. Park, and Y. C. Kim, "Effect of Synchronous Reluctance and Power Factor on HTS Synchronous Machine Design and Performance", *IEEE Transactions on Applied Superconductivity*, Vol.16, No.2, pp.1489-1492, June 2006.
- [5] P. C. Krause, O. Wasynczuk, and S. D. Sudhoff "Analysis of Electric Machinery and Drive Systems", Second Edition, IEEE Press, John Wiley & Sons, Inc., 2002.
- [6] A. Blondel, "Synchronous Motor and Converters- Part III", Translation by C. O. Mailloux, McGraw-Hill, 1913.
- [7] R. E. Doherty and C.A Nickle, "Synchronous Machines - Part I - An Extension of Blondel's Two-Reaction Theory", *AIEE Trans.*, Vol. 45, pp. 912-947, June 1926.
- [8] Li. Yan and Wang Dongmei, "Simulation of Synchronous Generator's Dynamic Operation Characteristics", *IEEE 10th International Conference on Electronic Measurement & Instruments (ICEMI) 2011*, Vol.2, pp.229-231, Aug. 2011.

- [9] A. A. Ansari and D. M. Deshpande, "Mathematical Model of Asynchronous Machine in MATLAB Simulink", *International Journal of Engineering Science and Technology*, 2010.
- [10] R. H. Park, "Two-Reaction Theory of Synchronous Machines-II", *A.I.E.E. Trans.*, Vol.52, No.2, pp.352-354, June 1933.
- [11] S. B. Crary, "Two-Reaction Theory of Synchronous Machines", *A.I.E.E. Trans.*, Vol.56, No.1, pp.27-36, Jan. 1937.
- [12] W. A. Lewis, "A Basic Analysis of Synchronous Machines – Part I", *AIEE Transactions, Power Apparatus and Systems, Part III*, Vol.77, No.3, pp.436-453, April 1958.
- [13] Xiaojun Z. Liu, George C. Verghese, Jeffrey H. Lang and Melih K. Onder, "Generalizing the Blondel-Park Transformation of Electrical Machines: Necessary and Sufficient Conditions", *IEEE Transactions on Circuits and Systems*, Vol.36, No.8, pp.1058-1067, Aug. 1989.
- [14] Y. H. Ku, "Rotating-Field Theory and General Analysis of Synchronous and induction Machines", *Institution Monograph*, No. 54, 1952.
- [15] Emmanuel Del. "An Algebraic and Geometric Look at Park Transformation: The Case of Permanent Magnets Synchronous Motor", *IEEE 1st International Conference on Electrical and Electronics Engineering (ICEEE) 2004*, pp. 573- 578, June 2004.
- [16] P. C. Krause and C. H. Thomas, "Simulation of Symmetrical Induction Machinery", *IEEE Transactions on Power Apparatus and Systems*, Vol.84, No.11, pp.1038-1053, Nov. 1965.

- [17] Burak Ozpineci and Leon M. Tolbert, "Simulink Implementation of Induction Machine Model- A Modular Approach", *Electric Machines and Drives Conference, IEMDC'03. IEEE International*, Vol. 2, pp. 728- 734, June 2003.
- [18] O. L. Okoro, "Matlab Simulation of Induction Machine with Saturable Leakage and Magnetizing Inductances", *The Pacific Journal of Science and Technology*, Vol. 5, April 2003.
- [19] K. L. Shi, T. F. Chan, Y. K. Wong and S. L. Ho, "Modelling and Simulation of the Three-Phase Induction Motor Using Simulink", *Int. J. Elect. Enging. Educ.*, Vol. 36, pp. 163-172. Manchester U.P. 1999.
- [20] L. Cociu, C. Haba and V. R. Cociu, "Particularities of Park Transformation in Special Cases", *2011 7th International Symposium on Advanced Topics in Electrical Engineering (ATEE)*, pp.1-6, May 2011.
- [21] Hans Knudsen, "Extended Park's Transformation for 2x3-Phase Synchronous Machine and Converter Phasor Model with Representation of AC Harmonics", *IEEE Transactions on Energy Conversion*, Vol.10, No.1, pp.126-132, March 1995.
- [22] D. Grenier and J. P. Louis, "Use of An Extension of the Park's Transformation to Determine Control Laws Applied to a Non-Sinusoidal Permanent Magnet Synchronous Motor", *Fifth European Conference on Power Electronics and Applications*, Vol.6, pp.32-37, Sept. 1993.
- [23] Chen Jikai, Li. Haoyu and Yang Shiyan, "Simulation Study for Harmonic Compensation System with Synchronous Machine Based on Park Transformation", *Power Electronics and Motion Control Conference, 2009. IPEMC '09. IEEE 6th International*, pp.1713-1718, May 2009.

- [24] M. Riaz, "Analogue Computer Representations of Synchronous Generators in Voltage-Regulation Studies", *AIEE Transactions, Power Apparatus and Systems, Part III*, Vol.75, No.3, pp.1178-1184, Dec. 1956.
- [25] R. J. Kerkman, P. C. Krause and T. A. Lipo, "Simulation of a Synchronous Machine with an Open Phase", *An International Quarterly*, Hemisphere Publishing Corporation, 1977.
- [26] Edson C. Bortoni, "Determination of direct-axis synchronous reactance of synchronous machines under operating conditions", *IEEE Power Engineering Review*, Vol.22, No.3, March 2002.
- [27] IEEE Guide, "Test Procedures for Synchronous Machines", IEEE Std. 115-1995.
- [28] IEC Standard, "Rotating Electrical Machines—Part 4: Methods for Determining Synchronous Machine Quantities from Tests", IEC 34-4: 1985.
- [29] ANSI/IEEE Standard 115A-1987, "Procedure for Obtaining Synchronous Machine Parameters by Standstill Frequency Response Testing".
- [30] J. C. Balda, M. F. Hadingham, R. E. Fairbairn, R. G. Harley, and E. Eitelberg, "Measurement of Synchronous Machine Parameters by a Modified Frequency Response Method- Part I: Theory", *IEEE Transactions on Energy Conversion*, Vol. EC-2, No. 4, pp. 646-651, December 1987.
- [31] J. C. Balda, R. E. Fairbairn, R. G. Harley, J. L. Rodgerson and E. Eitelberg, "Measurement of Synchronous Machine Parameters by a Modified Frequency Response

Method- Part II: Measured Results”, *IEEE Transactions on Energy Conversion*, Vol. EC-2, No. 4, pp. 652-657, December 1987.

[32] R. M. Saunders, “Synchronous-Machine Standstill Frequency-Response Test Data Analysis”, *IEEE Transactions on Energy Conversion*, Vol.6, No.3, pp.564-571, September 1991.

[33] F. P. Mello and J. R. Ribeiro, “Derivation of Synchronous Machine Parameters from Tests”, *IEEE Transactions on Power Apparatus and Systems*, Vol.96, No.4, pp. 1211-1218, July 1977.

[34] E. C. Bortoni and J. A. Jardini, “Identification of Synchronous Machine Parameters Using Load Rejection Test Data”, *IEEE Transactions on Energy Conversion*, Vol. 17, No. 2, pp.242-247, June 2002.

[35] S. D. Umans, J. A. Mallick and G. L. Wilson, “Modeling of Solid Rotor Turbogenerators- Part II”, *IEEE Transactions on Power Apparatus and Systems*, Vol. Pas-97, No.1, pp. 278-291, Jan./Feb.1978.

[36] M.-W. Naouar, E. Monmasson, and I. Slama-Belkhdja, “Identification of Synchronous Machine Parameters Using Hysteresis Based Current Controller”, *IECON 2006-32nd Annual Conference on IEEE Industrial Electronics*, pp.1357-1362, Nov. 2006.

[37] R. E. Doherty and O. E. Shirley, “Reactance of Synchronous Machines and its Applications”, *AIEE 34th Annual Convention*, pp. 1209-1340, June1918.

- [38] V. Karapetoff, "Variable Armature Leakage Reactance in Salient-Pole Synchronous Machines", *AIEE Trans*, pp. 729-734, May 1926.
- [39] R. H. Park and B. L. Robertson, "The Reactances of Synchronous Machines", *AIEE Trans.*, Vol. 47, No. 2, pp. 514-535, February 1928.
- [40] D. Harrington and J. Whittlesey, "The Analysis of Sudden-Short-Circuit Oscillograms of Steam-Turbine Generators", *AIEE Transactions, Power Apparatus and Systems, Part III*, Vol. 78, No. 3, pp. 551-562, August 1959.
- [41] R. E. Doherty and C. A. Nickle, "Three-Phase Short Circuit Synchronous Machines-V", *AIEE Trans.*, Vol. 49, No. 2, pp. 700-714, April 1930.
- [42] Sherwin H. Wright, "Determination of Synchronous Machine Constants by Test: reactances, resistances and time constants", *AIEE Trans.*, Vol. 50, No. 4, pp. 1331-1350, December 1931.
- [43] L. A. March and S. B. Crary, "Armature Leakage Reactance of Synchronous Machines", *AIEE Trans.*, Vol. 54, No. 4, pp. 378-381, April 1935.
- [44] A. M. El-Serafi and J. Wu, "A New Method for Determining the Armature Leakage Reactance of Synchronous Machines", *IEEE Transactions on Energy Conversion*, Vol. 6, No.1, pp.120-125, March 1991.
- [45] I. M. Canay, "Causes of Discrepancies on Calculation of Rotor Quantities and Exact Equivalent diagrams of the Synchronous Machine ", *IEEE Transactions on Power Apparatus and Systems*, Vol. Pas-88, No. 7, pp. 1114-1120, July 1969.

- [46] I. M. Canay, "Determination of Model Parameters for Synchronous Machines", *IEE Proceedings B, Electric Power Applications*, Vol.130, No. 2, pp. 86-94, March 1983.
- [47] I. M. Canay, "Determination of the Model Parameters of Machines from the Reactance Operators $X_d(p)$, $X_q(p)$ (Evaluation of Standstill Frequency Response Test)", *IEEE Transactions on Energy Conversion*, Vol. 8, No. 2, pp. 272-279, June 1993.
- [48] I. M. Canay, "Modelling of Alternating-Current Machines Having Multiple Rotor Circuits", *IEEE Transactions on Energy Conversion*, Vol. 8, No. 2, pp. 280-296, June 1993.
- [49] J. Verbeeck, R. Pintelon, and P. Guillaume, "Determination of Synchronous Machine Parameters Using Network Synthesis Techniques", *IEEE Transactions on Energy Conversion*, Vol. 14, No. 3, pp.310-314, September 1999.
- [50] L. Salvatore and M. Savino, "Experimental Determination of Synchronous Machine Parameters", *IEE Proceedings B, Electric Power Applications*, Vol.128, No. 4, pp.212-218, July 1981.
- [51] E. C. Shaffer and C. A. Gross, "Methods for Determining Linear Synchronous Machine Parameters", *Proceedings of the 26th Southeastern Symposium on System Theory*, pp.411-415, Mar 1994.
- [52] S. M. Zali, A. E. Ariffin, A. Mohamed, and A. Hussain, "Implementation of Synchronous Machine Parameter Derivation in Matlab", *TENCON 2000. Proceedings*, vol.1, pp.218-223, 2000.

- [53] K. Ide, S. Wakui, K. Shima and M. Takahashi "Analysis of Saturated Synchronous Reactances of Large Turbine Generator by Considering Cross-Magnetizing Reactances Using Finite Elements", *IEEE Transactions on Energy Conversion*, Vol. 14, No. 1, pp.66-71, March 1999.
- [54] Jukka Kaukonen, "Salient Pole Synchronous Machine Modelling in an Industrial Direct Torque Controlled Drive Application", Doctor of Science Thesis, Lappeenranta University of Technology, 1999.
- [55] J. Lidenholm and U. Lundin, "Estimation of Hydropower Generator Parameters through Field Simulations of Standard Tests", *IEEE Transactions on Energy Conversion*, Vol. 25, No. 4, pp.931-939, December 2010.
- [56] Y. Zhang, H. Wang, and Y. Li, "Study on Transient Characteristic of Large Hydro-Generator based on Field-Circuit Coupled Time-Stepping Finite Element Method", *2011 International Conference on Electrical Machines and Systems (ICEMS)*, pp.1-5, Aug. 2011.
- [57] Smarajit Ghosh, "Electrical Machines", First Impression, Dorling Kindersley (India) Pvt. Ltd, 2007.
- [58] A.E.Fitzgerald, C. Kingsley and Stephen D. Umans, "Electric Machinery", Fourth edition, Sixth edition, McGraw-Hill, 1983, 2003.
- [59] P. C. Sen, "Principles of Electric Machines and Power Electronics", John Wiley & Sons, Inc., 1989.
- [60] P. Kundur, "Power System Stability and Control", McGraw-Hill, Inc., 1994.

- [61] Stephen J. Chapman, "Electric Machinery Fundamentals", Third edition, McGraw-Hill, 1999.
- [62] B. S. Guru and H. R. Hiziroglu, "Electric Machinery and Transformers", Harcourt Brace Jovanovich (HBJ), Inc., 1988.
- [63] B. R. Prentice, "Fundamental Concepts of Synchronous Machine Reactances", *AIEE Trans.*, Vol. 56, No.12, pp.1-21, Dec. 1937.
- [64] E. W. Kimbark, "Power System Stability Vol. III: Synchronous Machines", John Wiley & Sons, Inc., 1956.
- [65] Westinghouse Electric Corporation, "Electric Transmission and Distribution", Reference book, East Pittsburgh, Pa, 1964.
- [66] J. Glover, S. Sarma and J. O. Thomas, "Power System Analysis and Design", Fourth edition, Thomson, TM., 2008.

Appendix A

Constants of Synchronous Machines

Table A.1 Typical constants of three-phase synchronous machines (Adapted from Refs. 42 and 65)

Type	X_d	X_q	X'_d	X''_d	X_2
2-Pole turbine generators	$\frac{1.10}{0.95 - 1.45}$	$\frac{1.07}{0.92 - 1.42}$	$\frac{0.15}{0.12 - 0.21}$	$\frac{0.09}{0.07 - 0.14}$	(= X''_d)
4-Pole turbine generators	$\frac{1.10}{1.00 - 1.45}$	$\frac{1.08}{0.97 - 1.42}$	$\frac{0.23}{0.20 - 0.28}$	$\frac{0.14}{0.12 - 0.17}$	(= X''_d)
Salient-pole gen. and motors (with dampers)	$\frac{1.15}{0.60 - 1.45}$	$\frac{0.75}{0.40 - 1.00}$	$\frac{0.37}{0.20 - 0.50}$	$\frac{0.24}{0.13 - 0.35}$	$\frac{0.24}{0.13 - 0.35}$
Salient-pole generators (without dampers)	$\frac{1.15}{0.60 - 1.45}$	$\frac{0.75}{0.40 - 0.95}$	$\frac{0.35}{0.20 - 0.45}$	(= X'_d)	$\frac{0.55}{0.30 - 0.70}$
Condensers	$\frac{1.80}{1.50 - 2.20}$	$\frac{1.15}{0.95 - 1.40}$	$\frac{0.40}{0.30 - 0.60}$	$\frac{0.25}{0.18 - 0.38}$	$\frac{0.24}{0.17 - 0.37}$

Table A.1 Cont.

Type	X_0^*	T'_{d0}	T'_d	T''_d^{\wedge}	T_a
2-Pole turbine generators	0.01-0.08	$\frac{4.40}{2.80 - 6.20}$	$\frac{0.60}{0.35 - 0.90}$	$\frac{0.035}{0.02 - 0.05}$	$\frac{0.09}{0.04 - 0.15}$
4-Pole turbine generators	0.015-0.14	$\frac{6.20}{4.00 - 9.20}$	$\frac{1.3}{0.80 - 1.80}$	$\frac{0.035}{0.02 - 0.05}$	$\frac{0.2}{0.15 - 0.35}$
Salient-pole gen. and motors (with dampers)	0.02-0.20	$\frac{5.60}{1.50 - 9.50}$	$\frac{1.80}{0.50 - 3.30}$	$\frac{0.035}{0.01 - 0.05}$	$\frac{0.15}{0.03 - 0.25}$
Salient-pole generators (without dampers)	0.04-0.25	$\frac{6.60}{3.00 - 10.50}$	$\frac{2.00}{1.00 - 3.30}$	—	$\frac{0.30}{0.10 - 0.50}$
Condensers	0.02-0.15	$\frac{9.00}{6.00 - 11.50}$	$\frac{2.00}{1.20 - 2.80}$	$\frac{0.035}{0.02 - 0.05}$	$\frac{0.17}{0.10 - 0.30}$

(*) X_0 varies so critically with stator winding pitch that an average value can hardly be given.

(\wedge) For single-phase machines (or three-phase machines designed for single-phase operation), T''_d may have much higher values than listed.

Appendix B

Three-Phase Short-Circuit at 0.6 pu of Rated Terminal Voltage

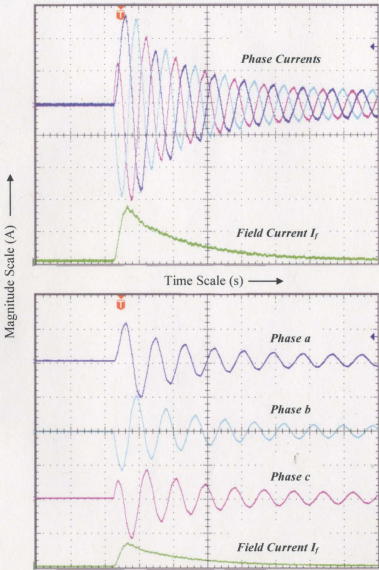


Fig. B.1 Typical oscillograms of sudden three-phase short-circuit at 0.6 pu rated voltage

